From www.bloodjournal.org at (D) TOKYO U MED LIB on March 25, 2009. For personal use only

Table 1. Efficiency of colony formation in soft agar

Cells*	Colony-forming efficiency, %	Average size of colonies, μm†
B5-EV1	0.7 ± 0.5	62.6 ± 1.5
B5-NIK#1	23.2 ± 2.0‡	236.2 ± 12.6‡
B5-NIK#2	18.9 ± 2.4‡	184.1 ± 19.8‡
B5-kd-NIK#1	1.5 ± 0.3	63.1 ± 1.4
B5-kd-NIK#2	1.3 ± 0.1	62.8 ± 1.8
h12-EV1	1.2 ± 0.3	60.5 ± 0.0
h12-NIK#1	12.8 ± 1.7‡	146.9 ± 4.6‡
h12-NIK#2	17.7 ± 1.7‡	154.9 ± 5.6‡
h12-kd-NIK#1	1.4 ± 1.0	61.5 ± 2.1
h12-kd-NIK#2	1.5 ± 0.4	62.5 ± 4.7
B5-EV1-EV2	1.2 ± 0.3	61.8 ± 1.1
B5-NIK#1-EV2	21.1 ± 1.0‡	193.8 ± 3.7‡
B5-NIK#2-EV2	14.3 ± 1.0‡	150.4 ± 8.7‡
h12-EV1-EV2	1.5 ± 0.7	60.8 ± 0.4
h12-NIK#1-EV2	12.3 ± 1.7‡	119.4 ± 5.6‡
h12-NIK#2-EV2	14.0 ± 1.8‡	160.3 ± 7.2‡
B5-EV1-SR-IκBα	1.5 ± 0.0	61.7 ± 0.5
B5-NIK#1-SR-IκBα	3.4 ± 0.0	64.8 ± 1.1
B5-NIK#2-SR-IκBα	3.9 ± 0.1	63.3 ± 0.4
h12-EV1-SR-IκBα	1.7 ± 1.0	61.3 ± 0.4
h12-NIK#1-SR-IκBα	2.7 ± 0.3	62.3 ± 0.1
h12-NIK#2-SR-IκBα	3.4 ± 1.4	61.4 ± 0.2

kd-NIK indicates catalytically inactive NIK; SR, super-repressor; EV1, empty vector for NIK or kd-NIK; and EV2, empty vector for SR-IκBα.

*Cells were inoculated in 0.33% soft agar and cultured for 3 weeks.

†Colonies larger than 60 μm were counted as positive. The sizes of more than 100 positive colonies were averaged.

‡$P < .05$ vs B5-EV1.

suppress NIK expression maximally, we used independently or in combination 2 shRNAs (NIKi-1 and -2) that target different *NIK* sequences and reduce NIK expression. The infected cells were then assayed for transcriptional activity by transient transfection with an NF-κB–dependent reporter gene (Figure 6A). Lentiviral expression of NIKi constructs resulted in suppression of NF-κB–dependent reporter gene expression in ATL cells when independently used, and the combined use of the 2 NIKi constructs (NIKi-1 and -2) was found to be more effective. We then examined ATL cells transduced with NIKi-1 and -2 constructs for the expression of endogenous NIK and specifically phosphorylated forms of p100, IκBα, and IKKs by immunoblotting (Figure 6B) and for NF-κB DNA binding activity by EMSA (Figure 6C). NIK expression in ATL cells was found to be down-regulated by the shRNA-mediated silencing (Figure 6B). As expected, p52 and phosphorylated p100 were also reduced by NIK depletion, and interestingly, phoshorylation of IκBα was also suppressed. This is consistent with the results observed in NIK-transduced rat fibroblasts that express the phoshorylated form of IκBα (Figure 5A), indicating that NIK, when aberrantly and stably expressed, induces phosphorylation of IκBα. In addition, NIK depletion suppressed phosphorylation of the serine residues in the activation loop of IKKs, suggesting a key role for NIK in constitutive activation of IKKs in ATL cells (Figure 6B). Moreover, depletion of NIK resulted in suppression of NF-κB DNA binding activity (Figure 6C). Super-shift assays revealed that DNA-binding of NF-κB components, p50, p52, RelA, and RelB was reduced by NIK depletion (Figure 6D). As shown previously, c-Rel was not detected in ATL cells.[34] We further investigated alterations in the expression of NF-κB target genes by NIK depletion. Vascular endothelial growth factor (VEGF), matrix metalloproteinase-9 (MMP-9), and intracellular adhesion molecule-1 (ICAM-1), the expression of which has been reported to be under the control of NF-κB,[35-37] are highly expressed in ATL cells and suggested to contribute to their invasive properties.[38-41] Quantitative RT-PCR studies reveal that depletion of NIK results in down-regulation of the expression of these NF-κB target genes (Figure 6E).

NIK regulates tumorigenicity of ATL cells in vivo

We finally investigated biologic effects of NIK depletion in ATL cells. NIK depletion did not significantly influence the growth of cells in culture (Figure 7A). We then examined whether depletion of NIK affects the tumorigenicity of ATL cells in a mouse model. NOD/SCID/γc^{null} mice were subcutaneously inoculated with ED-40515(−) cells that express Ctli or NIKi and are characterized in Figure 6B,C, and tumor formation was evaluated 2 weeks later. As expected, ED-40515(−) cells expressing Ctli efficiently formed large tumors, whereas tumors formed in mice inoculated with ED-40515(−) cells expressing NIKi were significantly smaller (Figure 7B-D), suggesting that NIK supports efficient tumor cell growth in vivo.

Discussion

Persistent activation of NF-κB has previously been reported to play an essential role in the growth and survival of specific cancer cell types, including ATL, H-RS, melanoma, and prostate cancer cells.[9,42-45] Inappropriate NF-κB activation can also contribute to the resistance to the apoptotic responses induced by certain anticancer drugs.[46] On the other hand, cancer cell apoptosis can be induced when persistent NF-κB activity is blocked by inhibitors, such as SR-IκBα, by drugs targeting IKK or the proteasome, via peptides targeting p50 or NEMO, and by double-stranded oligonucleotides containing NF-κB binding sites.[47,48] One problem with such inhibitors, however, is their lack of specificity to cancer cells because they also necessarily block normal NF-κB activation. Hence, it would be desirable to specifically inhibit NF-κB activation in cancer cells by identifying molecular targets in each cancer type. Virally transformed cancer cells express a virus-derived regulatory protein(s) that targets critical molecules in a variety of key signaling pathways. Cytokine autocrine loops or genetic alterations to genes regulating the NF-κB signaling mechanisms that lead to persistent NF-κB activation have also been identified in some cancer cells.[16,17,32,47,49] However, the mechanisms underlying persistent NF-κB activation in many types of cancer remain unknown.

Most primary ATL cells, although infected with HTLV-I, are characterized by the loss of viral protein expression, including Tax, probably because of the host immune surveillance during the long period of latency.[50] Nevertheless, NF-κB is strongly and persistently activated in ATL cells through IKK,[9] although the mechanism of IKK activation has remained unknown. The findings in our present study demonstrate the aberrant expression of *NIK* at the pretranslational level in ATL cells derived from 15 of 21 patients. This overexpression does not seem to correlate with the patients' age, sex, disease type, or percentage of abnormal lymphocytes (Table S1). Further studies will be required to clarify potentially NIK-independent NF-κB activation in the other 6 cases. The stable expression of functional NIK in fibroblasts, but not that of its catalytically inactive mutant, causes cellular transformation and persistent NF-κB activation with molecular features quite similar to those reported previously in ATL cells. These include the rapid

From www.bloodjournal.org at (D) TOKYO U MED LIB on March 25, 2009. For personal use only.

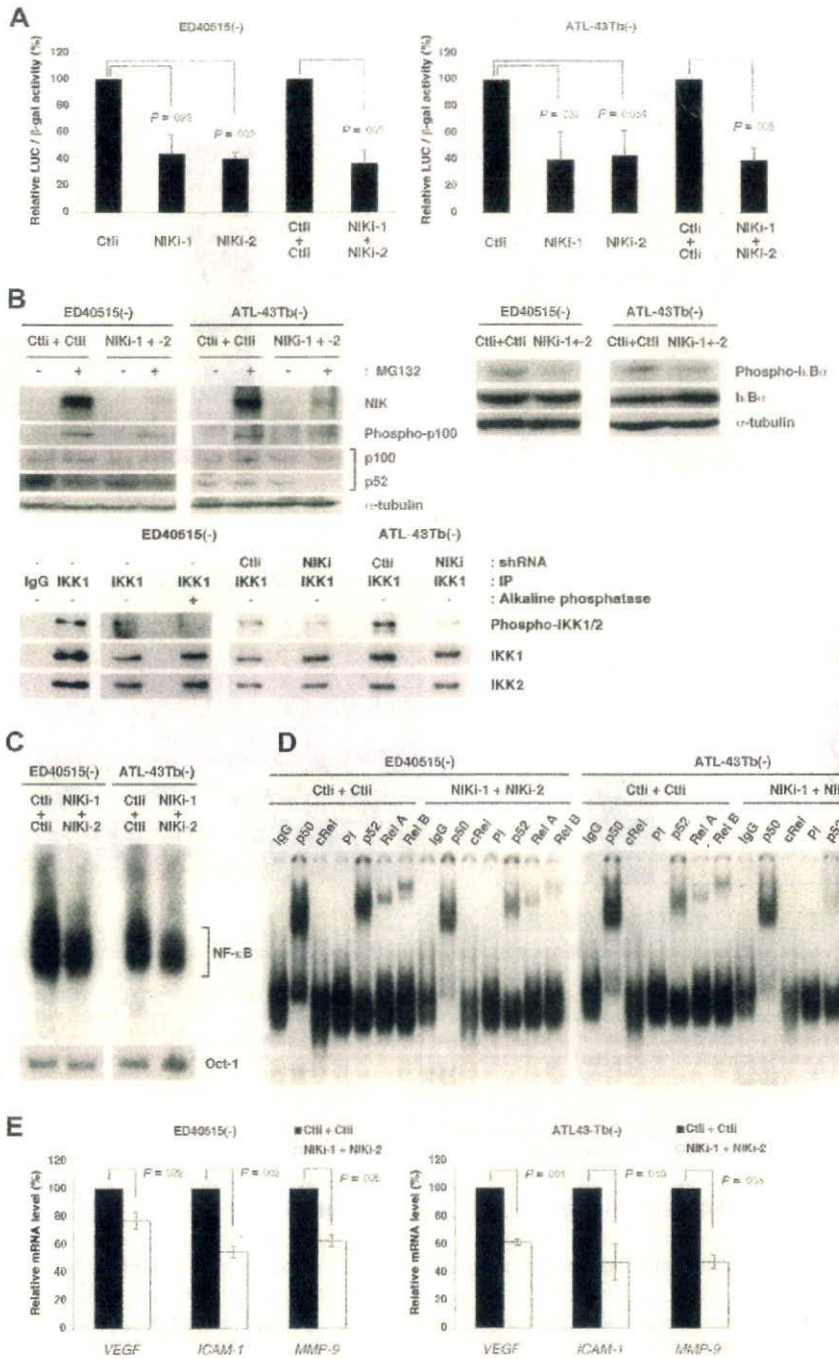

Figure 6. Depletion of NIK suppresses NF-κB-dependent transcription in ATL cells. (A) ED40515(−) and ATL-43Tb(−) cells were infected with lentiviral vectors expressing *Renilla luciferase* (Ctli) or *NIK*-specific shRNAs (NIKi-1 or NIKi-2). In parallel, ED40515(−) and ATL-43Tb(−) cells were infected with lentiviral vectors expressing Ctli or NIKi-1 shRNAs, and 24 hours later, these cells were super-infected with lentiviral vectors expressing Ctli or NIKi-2 shRNAs. Twenty-four hours after infection, cells were selected with puromycin for 2 days. Puromycin-resistant cells were then transfected with 2 μg of IgκCona-Luc and 2 μg EF1-LacZ. Luciferase (LUC) activity was determined 48 hours after transfection and normalized to β-gal activity. Relative luciferase activities, in comparison with control cells, 100 are shown. Data are expressed as mean plus or minus SD of 3 independent experiments. *P* values are versus control (Ctli). (B) Super-infected cells were treated with or without MG132 (20 μM) for 3 hours and subjected to SDS-PAGE and immunoblotting with anti-NIK (#4994), antiphosphorylated p100, or anti-α-tubulin antibodies. Whole-cell extracts (30 μg) from these cells were analyzed by SDS-PAGE and immunoblotting with antiphospho-IκBα, anti-IκBα, or anti-α-tubulin antibodies. Cytoplasmic extracts prepared from ED40515(−) cells infected or not with lentivirus were precleared and immunoprecipitation was performed, using anti-IKK1 monolconal antibody or its isotype IgG (IgG). After 3 washes with TNT buffer, immune complexes were treated or not with Shrimp Akaline Phosphatase (Takara Bio) and then subjected to SDS-PAGE and immunoblotting with antiphospho-IKK1/2, anti-IKK1, or anti-IKK2 antibodies. (C) A total of 5 μg of nuclear extracts prepared from lentivirus-infected cells shown in panel B were analyzed by EMSA, using oligonucleotides encoding the NF-κB–binding sequence or Oct-1–binding sequence as probes. (D) Nuclear extracts (5 μg) from lentivirus-infected cells shown in panel B were preincubated for 30 minutes with purified mouse IgG, anti-p50, anti-cRel antibody, preimmune (PI), anti-p50, anti-RelA or anti-RelB sera, and then subjected to EMSA with the NF-κB–specific probe. (E) Total RNAs from lentivirus-infected cells shown in panel B were examined by quantitative RT-PCR for *VEGF*, *ICAM-1*, and *MMP-9* mRNA levels. Each mRNA level was normalized to *18S* RNA. Relative mRNA levels, in comparison with control cells, 100 are shown. Data are expressed as mean plus or minus SD of 3 independent experiments. *P* values are versus control (Ctli + Ctli).

From www.bloodjournal.org at (D) TOKYO U MED LIB on March 25, 2009. For personal use only

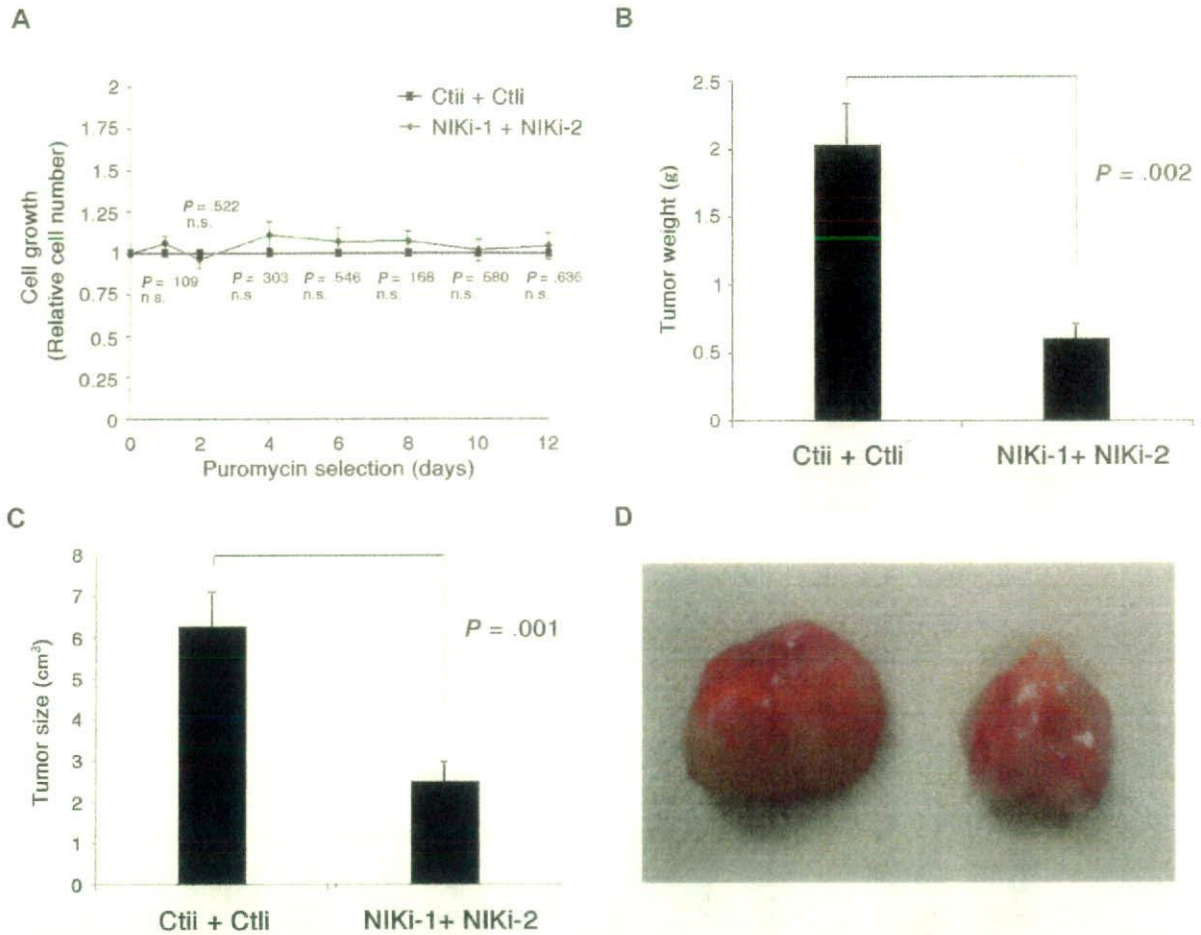

Figure 7. Depletion of NIK in ATL cells suppresses tumor formation in NOD-SCID/γc^{null} (NOG) mice. (A) Pools of ED40515(−) cells expressing Ctli or NIKi-1 and -2, shown in Figure 6B, C, D, and E, were analyzed for cell growth in vitro by the trypan blue staining method. Relative cell numbers, in comparison with control cells (arbitrarily set at 1), are shown. Data are expressed as mean plus or minus SD of 3 independent experiments. *P* values are vs control (Ctli + Ctii). n.s. indicates no significant difference. (B-D) NOG mice were inoculated subcutaneously in the postauricular region with the puromycin-resistant ED-40515(−) cells (5×10^6). Tumor formation in mice was evaluated 2 weeks after inoculation. Tumor weight (B) and size (C) relative to those of tumors formed in mice inoculated with ED40515(−) cells expressing Ctli are shown. (D) Photographs of tumors formed 2 weeks after cell inoculation. Each result was obtained from 5 different mice (means are shown [error bars]). *P* values are versus control (Ctli + Ctli).

loss of IKK activity after protein synthesis inhibition and the superinduction of IKK activity in the presence of MG132.[11] Moreover, RNA interference studies have also indicated that the deregulated NIK expression is the principal cause of constitutive NF-κB activation in ATL cells. In line with a previous report by Ramakrishnan et al, which showed that the induction of IκBα degradation by CD70, CD40 ligand, and BLyS/BAFF is dependent on the function of NIK,[18] we find in our present experiments that the stable expression of NIK induces IκBα phosphorylation and the formation of DNA binding complexes containing not only p50 and RelB, but also RelA both in wild-type and in NEMO-deficient rat fibroblasts. This indicates that NIK can stimulate the canonical pathway characterized by IκBα phosphorylation and RelA activation and that NIK does not require NEMO for it. Interestingly, the forced expression of SR-IκBα in these fibroblasts abolishes the transformed phenotype and suppresses constitutive NF-κB activity, with the p100 and p52 expression levels being diminished simultaneously, probably because p100 expression is largely dependent on NF-κB activity.[51] RelB expression is also known to be controlled by NF-κB,[52] suggesting that the noncanonical pathway of NF-κB activation does not work independently but rather coincides with NF-κB activation through the canonical pathway under stable conditions.

H-RS cells were also found to overexpress NIK, including its transcripts, in this study. Earlier reports have described 2 potential mechanisms of constitutive NF-κB activation in H-RS cells: persistent signaling from receptors that cause NF-κB activation, such as CD30, CD40, and RANK as well as a CD40-like molecule latent membrane protein 1 of the Epstein-Barr virus; and disruption of IκBα-dependent suppression resulting from the mutation of this gene.[32,48] The H-RS cell lines used in this study are Epstein-Barr virus-negative, and neither HDLM-2 nor L540 cells harbor mutations in their *IκB* genes. Indeed, CD30, CD40, and RANK were all found to be expressed in the H-RS cell lines used in this study, but we envisage that the aberrant expression of NIK is a distinct mechanism underlying the persistent NF-κB activation in these cells. It is partly because these TNF family receptor molecules, when stimulated or overexpressed transiently in cultured cells, elevate the NIK protein expression levels with a concomitant reduction in TRAF3 but do not increase *NIK* mRNA.[19,20]

From www.bloodjournal.org at (D) TOKYO U MED LIB on March 25, 2009. For personal use only.

Whereas the transient stimulation of a B-cell line with BAFF or anti-CD40 antibody stabilizes the NIK protein at the posttranslational level and does not up-regulate its mRNA expression,[20] NIK was observed to be constitutively overexpressed in ATL and H-RS cells at the pretranslational level. These differing mechanisms of NIK regulation may not be all that surprising, however, in light of the transient vs persistent nature of the activation of NF-κB. The barely detectable levels of steady-state NIK protein expression and its robust accumulation after proteasome inhibition in ATL and H-RS cells further suggest that the proteasome-dependent degradation of NIK occurs rapidly in tumor cells as in normal cells, although we cannot rule out the possibility that TNF family receptors known to be overexpressed in H-RS cells influence the stability of NIK to some extent. This point is currently very difficult to address because the protein amount of NIK in the absence of the proteasome inhibitor is quite limited. At least 3 mechanisms of pretranslational induction of NIK are plausible: the stabilization of *NIK* transcripts, transcriptional activation and/or amplification of the *NIK* gene. It should be noted that the stability of *NIK* mRNA in ATL cells was similar to that in control cells, suggesting that NIK expression is deregulated in ATL cells at the level of mRNA production. In this regard, we are currently analyzing the regulatory region of the *NIK* gene in normal and cancer cells.

We detected NIK in whole-cell lysates only when the cells themselves were treated with the proteasome inhibitor, MG132. It is possible that the expression of the NIK protein is tightly regulated under detectable levels in resting normal cells. However, in ATL and H-RS cells, enhanced NIK production, although still not detectable by simple immunoblotting, may be sufficient to cause its deregulated activity toward IKK. During the manuscript preparation, 2 reports demonstrated deregulated expression of NIK because of mutations in *TRAF3*, *CYLD*, or *NIK* itself in multiple myeloma cells.[16,17] In case of ATL cells, formation of a fusion protein after genomic rearrangement seems to be unlikely based on the apparently normal size of the protein. At present, the mechanism of overproduction of *NIK* mRNA in ATL cells remains to be determined, but the fluorescence in situ hybridization results suggest that aberrant NIK expression in ATL cells is not the result of genomic abnormalities, such as amplification or translocation.

Successful anticancer drug or gene therapies can be conducted in a number of ways, including the general administration of particular reagents that mechanistically work exclusively on cancer cells, or delivering conventional anticancer reagents specifically to cancer cells. The former strategy is likely to be more promising in the case of hematopoietic cancers. In this regard, NIK could be an attractive molecular target for ATL and Hodgkin lymphoma therapy, although the physiologic functions of NIK in human adults remain unknown. Suppressing high NF-κB activity levels by targeting NIK may also sensitize these cancer cells to commonly used anticancer agents.

Acknowledgments

The authors thank all of the ATL patients who donated blood samples for use in this study. Dr K. Yamaguchi and the Joint Study on Predisposing Factors of ATL Development for providing and analyzing sample blood, and the following researchers for donating invaluable reagents: Dr M. Maeda (Kyoto University, Kyoto, Japan) for the ED40515(−) and ATL-43Tb(−) cells, Dr D. Goeddel (Amgen, Thousand Oaks, CA) for *NIK* cDNAs, Dr N.R. Rice and Dr A. Israël (Institut Pasteur Paris, Paris, France) for p50, RelA, and RelB antisera, Dr T. Kitamura (University of Tokyo, Tokyo, Japan) for Plat-E cells, Dr I.S.Y. Chen (UCLA, Los Angeles, CA) for pHCMV-VSVG and pCMVΔR8.2 packaging plasmids, and Dr H. Miyoshi (RIKEN Tsukuba Institute, Tsukuba, Japan) for CS-CDF-CG-PRE plasmid. The authors also thank Dr G. Courtois (INSERM, Paris, France) and the members of the Department of Molecular Virology for helpful discussions.

This work was supported by research grants from the Ministry of Health and Labor Sciences (HIV/AIDS, H18-005) (Naoki Yamamoto) and from the Ministry of Education, Culture, Sports, Science and Technology of Japan (18390145; Naoki Yamamoto) and (17013029; S.Y.).

Authorship

Contribution: Y.S., T.S., and S.Y. designed the study; Y.S., Norio Yamamoto, H.S., V.J.M.B., Y.I., K.M., X.Q., I.I., J.I., and S.Y. carried out the research; M.Z.D. carried out the animal experiments; A.U. and T.W. collected and analyzed sample blood from ATL patients; T.M. contributed to lentiviral vector constructions; Y.S. and S.Y. analyzed the data; T.S., Naoki Yamamoto and S.Y. controlled the data; Y.S. and S.Y. wrote the paper; all authors checked the final version of the manuscript.

Conflict-of-interest disclosure: The authors declare no competing financial interests.

Correspondence: Shoji Yamaoka, Department of Molecular Virology, Graduate School of Medicine, Tokyo Medical and Dental University, 1-5-45, Yushima, Bunkyo-ku, Tokyo, 113-8510, Japan; e-mail: shojmmb@tmd.ac.jp.

References

1. Baldwin AS Jr. Series introduction: the transcription factor NF-kappaB and human disease. J Clin Invest. 2001;107:3-6.
2. Hayden MS, Ghosh S. Signaling to NF-kappaB. Genes Dev. 2004;18:2195-2224.
3. Xiao G, Rabson AB, Young W, Qing G, Qu Z. Alternative pathways of NF-kappaB activation: a double-edged sword in health and disease. Cytokine Growth Factor Rev. 2006;17:281-293.
4. Coope HJ, Atkinson PG, Huhse B, et al. CD40 regulates the processing of NF-kappaB2 p100 to p52. EMBO J. 2002;21:5375-5385.
5. Claudio E, Brown K, Park S, Wang H, Siebenlist U. BAFF-induced NEMO-independent processing of NF-kappa B2 in maturing B cells. Nat Immunol. 2002;3:958-965.
6. Karin M, Cao Y, Greten FR, Li ZW. NF-kappaB in cancer: from innocent bystander to major culprit. Nat Rev Cancer. 2002;2:301-310.
7. Jost PJ, Ruland J. Aberrant NF-{kappa}B signaling in lymphoma: mechanisms, consequences and therapeutic implications. Blood. 2006;109:2700-2707.
8. Ni H, Ergin M, Huang Q, et al. Analysis of expression of nuclear factor kappa B (NF-kappa B) in multiple myeloma: downregulation of NF-kappa B induces apoptosis. Br J Haematol. 2001;115:279-286.
9. Hironaka N, Mochida K, Mori N, Maeda M, Yamamoto N, Yamaoka S. Tax-independent constitutive IkappaB kinase activation in adult T-cell leukemia cells. Neoplasia. 2004;6:266-278.
10. Nonaka M, Horie R, Itoh K, Watanabe T, Yamamoto N, Yamaoka S. Aberrant NF-kappaB2/p52 expression in Hodgkin/Reed-Sternberg cells and CD30-transformed rat fibroblasts. Oncogene. 2005;24:3976-3986.
11. Miura H, Maeda M, Yamamoto N, Yamaoka S. Distinct IkappaB kinase regulation in adult T cell leukemia and HTLV-I-transformed cells. Exp Cell Res. 2005;308:29-40.
12. Dejardin E, Bonizzi G, Bellahcene A, Castronovo V, Merville MP, Bours V. Highly-expressed p100/p52 (NFKB2) sequesters other NF-kappa B-related proteins in the cytoplasm of human breast cancer cells. Oncogene. 1995;11:1835-1841.
13. Lessard L, Begin LR, Gleave ME, Mes-Masson AM, Saad F. Nuclear localization of nuclear factor-kappaB transcription factors in prostate cancer: an immunohistochemical study. Br J Cancer. 2005;93:1019-1023.
14. Chandler NM, Canete JJ, Callery MP. Increased

From www.bloodjournal.org at (D) TOKYO U MED LIB on March 25, 2009. For personal use only.

expression of NF-kappa B subunits in human pancreatic cancer cells. J Surg Res. 2004;118:9-14.

15. Bours V, Dejardin E, Goujon-Letawe F, Merville MP, Castronovo V. The NF-kappa B transcription factor and cancer: high expression of NF-kappa B- and I kappa B-related proteins in tumor cell lines. Biochem Pharmacol. 1994;47:145-149.
16. Annunziata CM, Davis RE, Demchenko Y, et al. Frequent engagement of the classical and alternative NF-kappaB pathways by diverse genetic abnormalities in multiple myeloma. Cancer Cell. 2007;12:115-130.
17. Keats JJ, Fonseca R, Chesi M, et al. Promiscuous mutations activate the noncanonical NF-kappaB pathway in multiple myeloma. Cancer Cell. 2007;12:131-144.
18. Ramakrishnan P, Wang W, Wallach D. Receptor-specific signaling for both the alternative and the canonical NF-kappaB activation pathways by NF-kappaB-inducing kinase. Immunity. 2004;21:477-489.
19. Liao G, Zhang M, Harhaj EW, Sun SC. Regulation of the NF-kappaB-inducing kinase by tumor necrosis factor receptor-associated factor 3-induced degradation. J Biol Chem. 2004;279:26243-26250.
20. Qing G, Qu Z, Xiao G. Stabilization of basally translated NF-kappaB-inducing kinase (NIK) protein functions as a molecular switch of processing of NF-kappaB2 p100. J Biol Chem. 2005;280:40578-40582.
21. Maeda M, Shimizu A, Ikuta K, et al. Origin of human T-lymphotrophic virus I-positive T cell lines in adult T cell leukemia: analysis of T cell receptor gene rearrangement. J Exp Med. 1985;162:2169-2174.
22. Yagi H, Nomura T, Nakamura K, et al. Crucial role of FOXP3 in the development and function of human $CD25^+CD4^+$ regulatory T cells. Int Immunol. 2004;16:1643-1656.
23. Sugamura K, Fujii M, Kannagi M, Sakitani M, Takeuchi M, Hinuma Y. Cell surface phenotypes and expression of viral antigens of various human cell lines carrying human T-cell leukemia virus. Int J Cancer. 1984;34:221-228.
24. Foley GE, Lazarus H, Farber S, Uzman BG, Boone BG, McCarthy RE. Continuous cultured human lymphoblasts from peripheral blood of a child with acute leukemia. Cancer. 1965;18:522-529.
25. Weiss A, Wiskocil RL, Stobo JD. The role of T3 surface molecules in the activation of human T cells: a two-stimulus requirement for IL 2 production reflects events occurring at pre-translational level. J Immunol. 1984;133:123-128.
26. Yamaoka S, Courtois G, Bessia C, et al. Complementation cloning of NEMO, a component of the IkappaB kinase complex essential for NF-kappaB activation. Cell. 1998;93:1231-1240.
27. Chinanonwait N, Miura H, Yamamoto N, Yamaoka S. A recessive mutant cell line with a constitutive IkappaB kinase activity. FEBS Lett. 2002;531:553-560.
28. Morita S, Kojima T, Kitamura T. Plat-E: an efficient and stable system for transient packaging of retroviruses. Gene Ther. 2000;7:1063-1066.
29. Yamaoka S, Inoue H, Sakurai M, et al. Constitutive activation of NF-kappa B is essential for transformation of rat fibroblasts by the human T-cell leukemia virus type I Tax protein. EMBO J. 1996;15:873-887.
30. Munoz E, Courtois G, Veschambre P, Jalinot P, Israël A. Tax induces nuclear translocation of NF-kappa B through dissociation of cytoplasmic complexes containing p105 or p100 but does not induce degradation of I kappa B alpha/MAD3. J Virol. 1994;68:8035-8044.
31. Dewan MZ, Terashima K, Taruishi M, et al. Rapid tumor formation of human T-cell leukemia virus type 1-infected cell lines in novel NOD-SCID/γc^{null} mice: suppression by an inhibitor against NF-κB. J Virol. 2003;77:5286-5294.
32. Krappmann D, Emmerich F, Kordes U, Scharschmidt E, Dorken B, Scheidereit C. Molecular mechanisms of constitutive NF-kappaB/Rel activation in Hodgkin/Reed-Sternberg cells. Oncogene. 1999;18:943-953.
33. Wood KM, Roff M, Hay RT. Defective IkappaBalpha in Hodgkin cell lines with constitutively active NF-kappaB. Oncogene. 1998;16:2131-2139.
34. Mori N, Fujii M, Ikeda S, et al. Constitutive activation of NF-kappaB in primary adult T-cell leukemia cells. Blood. 1999;93:2360-2368.
35. Yemelyanov A, Gasparian A, Lindholm P, et al. Effects of IKK inhibitor PS1145 on NF-kappaB function, proliferation, apoptosis and invasion activity in prostate carcinoma cells. Oncogene. 2006;25:387-398.
36. Farina AR, Tacconelli A, Vacca A, Maroder M, Gulino A, Mackay AR. Transcriptional up-regulation of matrix metalloproteinase-9 expression during spontaneous epithelial to neuroblast phenotype conversion by SK-N-SH neuroblastoma cells, involved in enhanced invasivity, depends upon GT-box and nuclear factor kappaB elements. Cell Growth Differ. 1999;10:353-367.
37. Collins T, Read MA, Neish AS, Whitley MZ, Thanos D, Maniatis T. Transcriptional regulation of endothelial cell adhesion molecules: NF-kappa B and cytokine-inducible enhancers. FASEB J. 1995;9:899-909.
38. El-Sabban ME, Merhi RA, Haidar HA, et al. Human T-cell lymphotropic virus type 1-transformed cells induce angiogenesis and establish functional gap junctions with endothelial cells. Blood. 2002;99:3383-3389.
39. Mori N, Sato H, Hayashibara T, et al. Human T-cell leukemia virus type I Tax transactivates the matrix metalloproteinase-9 gene: potential role in mediating adult T-cell leukemia invasiveness. Blood. 2002;99:1341-1349.
40. Hayashibara T, Yamada Y, Onimaru Y, et al. Matrix metalloproteinase-9 and vascular endothelial growth factor: a possible link in adult T-cell leukaemia cell invasion. Br J Haematol. 2002;116:94-102.
41. Fukudome K, Furuse M, Fukuhara N, Orita T, Hinuma Y. Strong induction of ICAM-1 in human T cells transformed by human T-cell leukemia virus type 1 and depression of ICAM-1 or LFA-1 in adult T-cell leukemia-derived cell lines. Int J Cancer. 1992;52:418-427.
42. Mori N, Yamada Y, Ikeda S, et al. Bay 11–7082 inhibits transcription factor NF-kappaB and induces apoptosis of HTLV-I-infected T-cell lines and primary adult T-cell leukemia cells. Blood. 2002;100:1828-1834.
43. Bargou RC, Emmerich F, Krappmann D, et al. Constitutive nuclear factor-kappaB-RelA activation is required for proliferation and survival of Hodgkin's disease tumor cells. J Clin Invest. 1997;100:2961-2969.
44. Yang J, Amiri KI, Burke JR, Schmid JA, Richmond A. BMS-345541 targets inhibitor of kappaB kinase and induces apoptosis in melanoma: involvement of nuclear factor kappaB and mitochondria pathways. Clin Cancer Res. 2006;12:950-960.
45. Gasparian AV, Yao YJ, Kowalczyk D, et al. The role of IKK in constitutive activation of NF-kappaB transcription factor in prostate carcinoma cells. J Cell Sci. 2002;115:141-151.
46. Wang CY, Cusack JC Jr, Liu R, Baldwin AS Jr. Control of inducible chemoresistance: enhanced anti-tumor therapy through increased apoptosis by inhibition of NF-kappaB. Nat Med. 1999;5:412-417.
47. Gilmore TD, Herscovitch M. Inhibitors of NF-kappaB signaling: 785 and counting. Oncogene. 2006;25:6887-6899.
48. Braun T, Carvalho G, Fabre C, Grosjean J, Fenaux P, Kroemer G. Targeting NF-kappaB in hematologic malignancies. Cell Death Differ. 2006;13:748-758.
49. Courtois G, Gilmore TD. Mutations in the NF-kappaB signaling pathway: implications for human disease. Oncogene. 2006;25:6831-6843.
50. Sun SC, Yamaoka S. Activation of NF-kappaB by HTLV-I and implications for cell transformation. Oncogene. 2005;24:5952-5964.
51. Liptay S, Schmid RM, Nabel EG, Nabel GJ. Transcriptional regulation of NF-kappa B2: evidence for kappa B-mediated positive and negative autoregulation. Mol Cell Biol. 1994;14:7695-7703.
52. Bren GD, Solan NJ, Miyoshi H, Pennington KN, Pobst LJ, Paya CV. Transcription of the RelB gene is regulated by NF-kappaB. Oncogene. 2001;20:7722-7733.

Biochemical and Biophysical Research Communications 376 (2008) 310–314

Contents lists available at ScienceDirect

Biochemical and Biophysical Research Communications

journal homepage: www.elsevier.com/locate/ybbrc

Identification of the RelA domain responsible for action of a new NF-κB inhibitor DHMEQ

Mariko Watanabe [a,1], Makoto Nakashima [a,1], Tomiteru Togano [a], Masaaki Higashihara [a], Toshiki Watanabe [b], Kazuo Umezawa [c], Ryouichi Horie [a,*]

[a] Department of Hematology, School of Medicine, Kitasato University, 1-15-1 Kitasato, Sagamihara, Kanagawa 228-8555, Japan
[b] Laboratory of Tumor Cell Biology, Department of Medical Genome Sciences, Graduate School of Frontier Sciences, University of Tokyo, 4-6-1 Shirokanedai, Minato-ku, Tokyo 108-8639, Japan
[c] Department of Applied Chemistry, Faculty of Science and Technology, Keio University, 3-14-1 Hiyoshi, Kohoku-ku, Yokohama, Kanagawa 223-0061, Japan

ARTICLE INFO

Article history:
Received 24 August 2008
Available online 7 September 2008

Keywords:
NF-κB inhibitor
DHMEQ
RelA
p50

ABSTRACT

A new NF-κB inhibitor dehydroxymethylepoxyquinomicin (DHMEQ) has a potential to be applied to clinical medicine as an anti-cancer and anti-inflammatory agent. DHMEQ inhibits localization of NF-κB in the nucleus and the inhibitory effect by DHMEQ is more potent on p50/RelA than on p50 homodimer. However, a molecular target of DHMEQ is unknown. In this study, we identified residues CEGRSAGSI, which appear in RelA (amino acids 38–46), c-Rel (28–36), and RelB (144–152), but not in p50 and p52, as a target of DHMEQ. As a possible mechanism, we propose that DHMEQ accesses CEGRSAGSI domain recognizing RSAGSI structure and directly binds to cysteine. This target domain appears to be unique among mammalian proteins. The results obtained in this study may provide better understanding of the action of DHMEQ and a key for developing a new NF-κB inhibitor with more potent activity.

© 2008 Elsevier Inc. All rights reserved.

Dehydroxymethylepoxyquinomicin (DHMEQ) is a new NF-κB inhibitor that is a 5-dehydroxymethyl derivative of the novel compound epoxyquinomicin C with a 4-hydroxy-5,6-epoxycyclohexenone structure like panepoxydone [1]. NF-κB represents a family of inducible transcription factors and activation of NF-κB has been connected with resistance against apoptosis and tumorigenesis [2,3]. Accumulating evidences indicate that DHMEQ is a promising compound to be applied to clinical medicine as an anti-cancer and anti-inflammatory agent [4].

We have shown that DHMEQ acts at the downstream of IκB kinase and inhibits localization of NF-κB in the nucleus. DHMEQ did not inhibit nuclear localization of SV-40 large T antigen or Smad2, suggesting that DHMEQ does not target the general mechanism involved in nuclear localization, but targets some other mechanism that is more specific to the NF-κB pathway [5]. Furthermore, our previous studies showed that DHMEQ inhibits constitutive NF-κB activity consisting of p50/RelA (p65), but its effect is less potent against p50 homodimer [6,7]. This specific action of DHMEQ may explain why DHMEQ can effectively induce apoptosis in cancer cells with constitutive NF-κB activity consisting of p50/RelA, but does not affect normal resting lymphocytes, whose NF-κB activity consists mainly of p50 homodimer without RelA. However, the molecular target of DHMEQ and the reason, which explains difference in the specificity of DHMEQ between p50/RelA and p50 homodimer are entirely unknown.

In this study, we identified a molecular target of DHMEQ and elucidated the reason for the difference in the specificity of DHMEQ between p50/RelA and p50 homodimer by comparing the RelA domain with the corresponding domain in p50 as well as other NF-κB family proteins.

Materials and methods

Cell cultures. HeLa cell line was obtained from the Japanese Cancer Research Resources Bank (Tokyo, Japan). KMH2 cell line was purchased from the German Collection of Microorganisms and Cell Cultures (Braunschweig, Germany). The TL-Om1 cell line was a gift from Dr. K. Sugamura, Tohoku University. Non-adherent cell lines were cultured in RPMI 1640 medium and adherent cells were cultured in Dulbecco's modified Eagle's medium (DMEM) with supplementation of recommended concentrations of fetal bovine serum (FBS) and antibiotics.

Chemicals. We used (−)-DHMEQ, which is 10 times more potent than (+)-DHMEQ. (−)-DHMEQ was synthesized as previously described [1]. DHMEQ was dissolved in dimethyl sulfoxide (DMSO) for use in experiments. Human TNF-α was purchased from PEPRO TECH, INC. (Rocky Hill, NJ, USA). Dithiothreitol (DTT) and isopropyl

* Corresponding author. Fax: +81 42 778 8441.
E-mail address: rhorie@med.kitasato-u.ac.jp (R. Horie).
[1] These authors equally contributed to this work.

0006-291X/$ - see front matter © 2008 Elsevier Inc. All rights reserved.
doi:10.1016/j.bbrc.2008.08.148

1-thio-β-D-galactoside (IPTG) were purchased from Promega (Madison, WI, USA).

Plasmids and mutagenesis. Wild-type human RelA cDNA was cloned by polymerase chain reaction (PCR) using cDNA from TL-Om1 cells and was then inserted into pEGFP-N1 expression vector (Clontech, Mountain View, CA, USA). N-terminal deletion mutants of RelA were prepared by PCR using wild-type RelA cDNA and were then cloned into pEGFP-C1 expression vector (Clontech). Wild-type human cDNAs for p50, p52, and c-Rel were cloned by PCR using cDNA from KMH2 cells and inserted into pGFPN-1 expression vector (Clontech). The expression vectors for IκBα and RelB cDNA were generous gifts from Dr. J. Inoue at Tokyo University. Amino acid numbers corresponding to the region cloned into the expression vectors and the National Center for Biotechnology Information (NCBI) accession numbers. of each corresponding protein are as follows: RelA (amino acids 1–551, NCBI Accession No. NM_021975), c-Rel (amino acids 1–619, NCBI Accession No. NM_002908), p50 (amino acids 1–436, NCBI Accession No. NM_003998) and p52 (amino acids 1–405, NCBI Accession No. NM_001077494).

Using the method for mutagenesis by Kunkel et al., we obtained the expression vectors that express mutant protein: RelAmut [RelA RSAGSI (amino acids 41–46) was replaced by the corresponding domain of p50 PSHGGL (amino acids 65–70)], RelAC38S (amino acid 38 cysteine of RelA was replaced by serine), and p50mut (p50 PSHGGL was replaced by corresponding domain of RelA RSAGSI) [8].

Immunofluorescence. To observe the localization of NF-κB family proteins, 1×10^5 of HeLa cells were transfected with 1 μg of Green Fluorescent Protein (GFP) fused vector plasmid and 1 μg of IκBα expression vector using Lipofectamine 2000 reagent (Invitrogen, Carlsbad, CA, USA) according to the manufacturer's instructions. HeLa cells seeded onto poly-L-lysine-coated culture coverglass (MATSUNAMI, Osaka, Japan) served for transfection. After an additional 18 h of culturing, cells were pretreated with or without 10 μg/ml of DHMEQ for 1 h before stimulation with or without 20 ng/ml of TNF-α for 15 min. Subsequently, cells were washed in phosphate-buffered saline (PBS) three times, fixed in 4% paraformaldehyde phosphate buffer solution (Wako, Osaka, Japan) for 10 min and washed in PBS three times. After final washing, the coverslips were dried and mounted on slides with a Perma Fluoro anti-fade reagent (Therme Shandon Co., Pittsburgh, PA, USA). Fluorescence signals were detected using confocal microscopy (Radiance 2000, Bio-Rad Laboratories, Hercules, CA, USA).

Immunohistochemistry. Cells were immunostained with antibodies and fluorescence signals were detected using confocal microscopy. Cytospin samples were prepared using 1×10^5 cells and were first washed three times with PBS. Cells were then fixed with methanol or 10% paraformaldehyde for 10 min at room temperature and washed three times in PBS. Samples were incubated with primary antibody at the concentration of 5 μg/ml at 4 °C overnight and washed with PBS three times. After incubation with fluorescence-labeled secondary antibody for 30 min at 37 °C, samples were washed three times in PBS and covered with a Perma Fluoro anti-fade reagent (Therme Shandon Co.). Fluorescence signals were detected using confocal microscopy (Radiance 2000) (Bio-Rad Laboratories). Antibodies used were as follows: anti-NF-κB p65 SUBUNIT mouse monoclonal antibody (Chemicon International, Temecula, CA, USA) and goat anti-mouse IgG FITC conjugated antibody (Santa Cruz Biotechnology, Inc.).

Production of glutathione S-transferase (GST) fusion protein. Human RelA cDNA corresponding to amino acids 1–327 was amplified by PCR using wild-type RelA expression vector as a template and then cloned into pGEX-5X-1 vector (GE Healthcare). We created expression vectors for amino acids 1–327 of RelAC38S using the same strategy. Recombinant proteins were expressed in *Escherichia coli DH5α* (Takara Kyoto, Japan) as GST fusion proteins at 30 °C for 4 h under induction with 0.1 mM IPTG. Glutathione S-transferase and GST fusion proteins were prepared by standard methods [9].

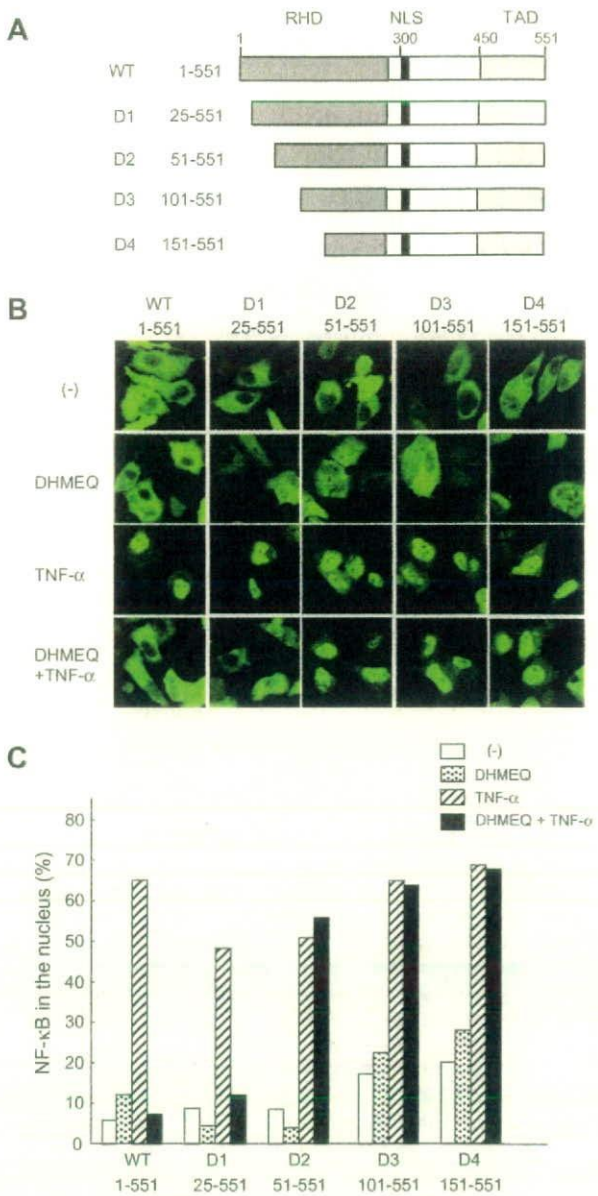

Fig. 1. The N-terminus of RelA (amino acids 25–50) is responsible for the inhibition of the nuclear localization of RelA by DHMEQ. (A) Primary domain structure of wild-type and its truncation constructs of RelA. The location of Rel homology domain (RHD), nuclear localization signal (NLS), and trans activation domain (TAD) are presented according to the previous study [18]. The numbers on the left and those on the top indicate the amino acid numbers of RelA. (B) Fluorescence analysis to determine the RelA domain responsible for the inhibition of the TNF-α-mediated localization of RelA in the nucleus by DHMEQ. HeLa cells were transfected with the indicated cDNA expression vectors for GFP fusion constructs and the expression vector for IκBα. After 18 h, cells were stimulated with or without 20 ng/ml of TNF-α for 15 min under pretreatment with or without 10 μg/ml of DHMEQ for 1 h as indicated on the left. Location of the constructs visualized by autofluorescence of GFP was observed by confocal laser microscopy. Representative distribution patterns that characterize each group are presented as representative figures. The RelA constructs used are indicated on the top. (C) Quantitative analysis. For quantification, 300 cells were scored for fluorescence location in the nucleus. The data are representative of triplicate experiments.

The recombinant proteins were immobilized onto GST-binding resin (Novagen, Madison, WI, USA) and served for the experiments after washing with PBS five times.

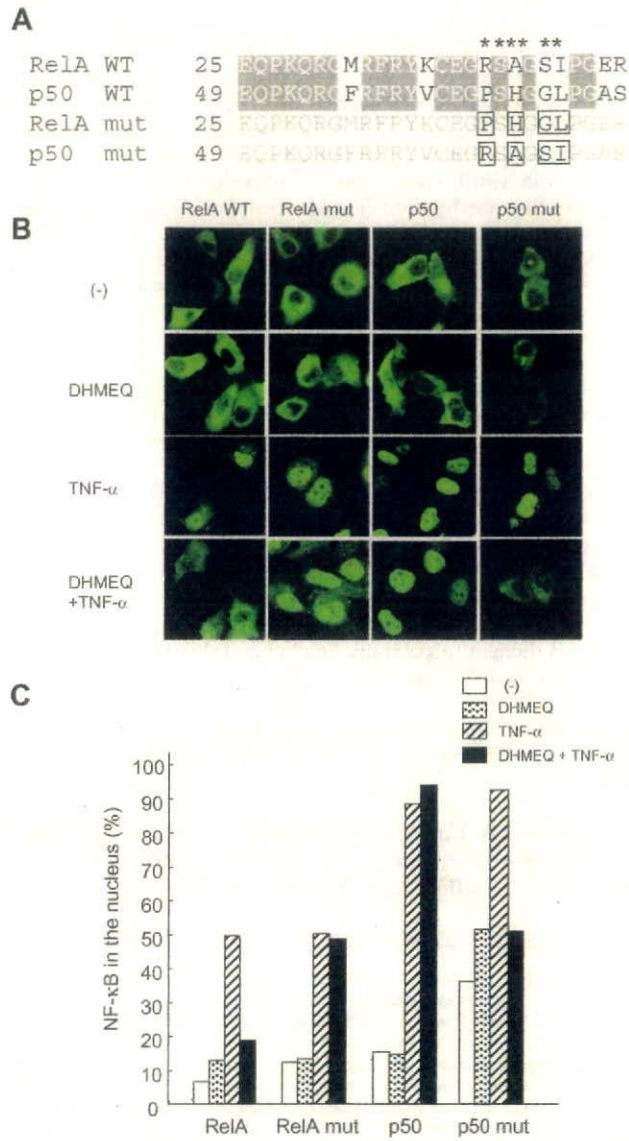

Fig. 2. The domain RSAGSI (amino acids 41–46) of RelA is responsible for the DHMEQ-mediated inhibition of the nuclear localization of RelA and the differentiation of the effect of DHMEQ on p50. (A) Comparison of the amino acid alignment of RelA, p50, and their mutants. RelA RSAGSI (amino acids 41–46) and p50 PSHGGL (amino acids 65–70), which are indicated by asterisks, are less conserved within the domain corresponding to that of RelA responsible for DHMEQ action (amino acids 25–50). Conserved residues between RelA and p50 are indicated on a gray background. The structures of RelAmut and p50mut are described in the Materials and methods section. Amino acid residues replaced are indicated by open squares. The numbers on the left indicate the amino acid number of each protein. (B) Fluorescence analysis to determine the domain that differentiates the action of DHMEQ on RelA and p50. HeLa cells were transfected with the indicated cDNA expression vectors for GFP fusion constructs and the expression vector for IκBα, treated, and observed as described in the legend for Fig. 1B. Constructs used are indicated on the top. (C) Quantitative analysis. Quantification was done as described in the legend for Fig. 1C. The data are representative of triplicate experiments.

Results and discussion

Identification of the RelA domain responsible for DHMEQ-mediated inhibition of nuclear localization of RelA

Previous observation indicated that DHMEQ does not target the general mechanism involved in nuclear transportation, but targets some other mechanism that is more specific to NF-κB [5]. Therefore, we first examined the effect of DHMEQ on RelA deletion mutants, which lack an N-terminus and contain residues spanning 25–551 (D1), 51–551 (D2), 101–551 (D3), and 151–551 (D4) of RelA (Fig. 1A). These RelA mutants and wild-type RelA were constructed as GFP fusion proteins and transfected into HeLa cells. Expression of wild-type RelA in HeLa cells was characterized by

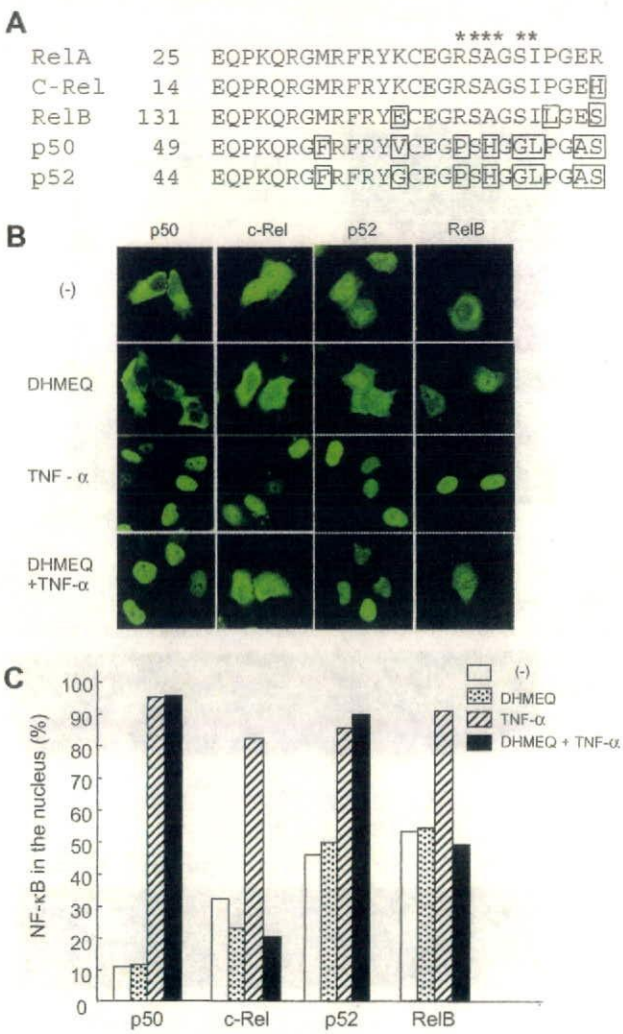

Fig. 3. DHMEQ inhibits the localization of c-Rel and RelB, which retain RelA RSAGSI, but not that of p52, which has p50 PSHGGL. (A) Comparison of the amino acid alignment of RelA, c-Rel, RelB, p50, and p52. Amino acid alignment corresponding to RelA RSAGSI (amino acids 41–46) is indicated by asterisks. Residues not conserved, when compared with RelA, are indicated by open squares. The numbers on the left indicate the amino acid number of each protein. (B) Fluorescence analysis to differentiate the response for the action of DHMEQ on NF-κB family proteins. HeLa cells were transfected with the indicated cDNA expression vectors for GFP fusion constructs and the expression vector for IκBα, treated, and observed as described in the legend for Fig. 1B. Constructs used are indicated on the top. (C) Quantitative analysis. Quantification was done as described in the legend for Fig. 1C. The data are representative of triplicate experiments.

predominant cytoplasmic distribution, as previously reported [5]. We cotransfected RelA constructs and IκBα, because transfection of RelA D4 alone caused nuclear localization (data not shown), which might be explained by the loss of IκBα induction ability, as previously reported [10]. Under this experimental condition, transfection of wild-type and each deletion mutant was characterized by predominant cytoplasmic distribution (Fig. 1B, top panel). Treatment with DHMEQ did not affect this distribution pattern (Fig. 1B, second panel). TNF-α stimulation changed their distribution from a cytoplasmic to a nuclear pattern (Fig. 1B, third panel). Pretreatment with DHMEQ inhibited the TNF-α-mediated nuclear localization when wild-type and D1 constructs were used, whereas DHMEQ did not inhibit nuclear localization when D2, D3, and D4 constructs were used (Fig. 1B, bottom panels; Fig. 1C). These observations indicate that the RelA domain, which is responsible for DHMEQ-mediated inhibition of nuclear localization of NF-κB, resides within residues 25–50 of RelA.

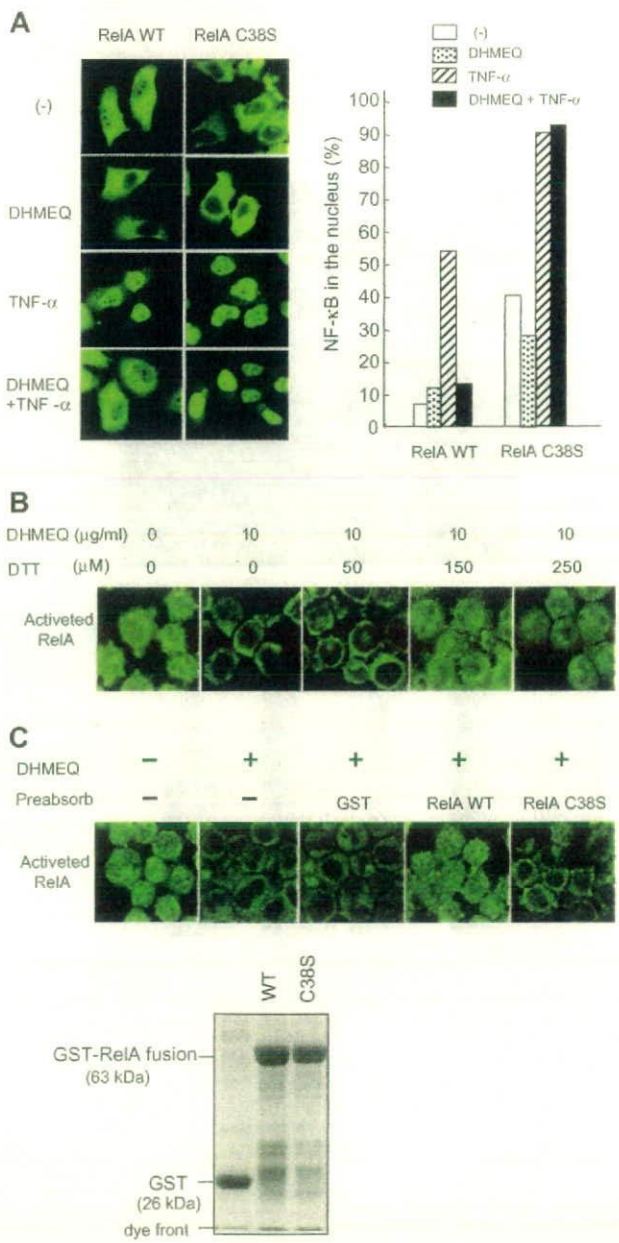

The RelA domain RSAGSI differentiates the effect by DHMEQ on RelA and p50

Our previous observation showed that DHMEQ inhibits constitutive NF-κB activity consisting of p50/RelA, but its effect is less potent against p50 homodimer [6,7]. To identify the amino acid residues, which are responsible for the different effect by DHMEQ on RelA and p50, we analyzed the amino acid homology between RelA and p50 and took notice of the domain RSAGSI spanning residues 41–46 of RelA (Fig. 2A). Transfection of GFP-fused p50 alone in Hela cells caused nuclear localization (data not shown). A previous report showed that IκBα associates not only with RelA, but also with p50 [11]. Therefore, we cotransfected expression plasmids for GFP-fused RelA, p50 or their mutants with that for IκBα, which enabled us to observe the TNF-α-dependent change in their distribution. Replacement of RSAGSI (amino acids 41–46) of RelA with the corresponding domain of p50 PSHGGL (amino acids 65–70), which is indicated as RelAmut, abolished the effect of DHMEQ (Fig. 2B, second row from the left; Fig. 2C). Inversely, replacement of p50 PSHGGL with the corresponding domain of RelA (RSAGSI), which is indicated as p50mut, recovered the effect of DHMEQ (Fig. 2B, third and fourth rows from the left; Fig. 2C). These observations indicate that the domain RSAGSI spanning residues 41–46 of RelA is responsible for the DHMEQ-mediated inhibition of nuclear localization of RelA and the differentiation of the effect of DHMEQ on p50.

The result indicates that inhibitory effect of DHMEQ operates if at least one partner of dimeric NF-κB complex is RelA. This selective action of DHMEQ appears to be important for its specificity to exert anti-cancer and anti-inflammatory activity, because p50/RelA plays a major role in cancer cell growth and inflammatory activity, whereas p50 homodimer, which lacks transactivation activity, is thought to generally function as transcriptional repressors for p50/RelA activity [12].

DHMEQ inhibits TNF-mediated localization of c-Rel and RelB, which retain RelA RSAGSI, but not that of p52 having p50 PSHGGL in the nucleus

RelA RSAGSI is shared among RelA, c-Rel, and RelB, whereas p50 PSHGGL is shared between p50 and p52 (Fig. 3A). We next examined the effect of DHMEQ on c-Rel, RelB, and p52. As was the case

Fig. 4. DHMEQ directly targets cysteine 38 of RelA. (A) Fluorescence analysis to observe the effect of replacing cysteine 38 of RelA with serine (left). HeLa cells were transfected with the indicated cDNA expression vectors for GFP fusion constructs, treated, and observed as described in the legend for Fig. 1B. Constructs used are indicated on the top. Quantitative analysis (right). For quantification, 300 cells were scored for fluorescence location in the nucleus. The data are representative of triplicate experiments. (B) Immunofluorescence analysis to determine the effect of DTT on the DHMEQ-mediated inhibition of the translocation of RelA in the nucleus. KMH2 cells with strong and constitutive NF-κB activity were treated with or without 10 μg/ml of DHMEQ for 5 h under pretreatment with DTT for 2 h at culture conditions of 37 °C, 5% CO_2. Cells were subjected to indirect immunofluorescence analysis with antibody for activated RelA, which recognizes RelA NLS, and FITC-conjugated secondary antibody. (C) Nuclear localization of activated RelA was abolished by pre-absorption of DHMEQ with wild-type RelA, but not with RelA C38S, in KMH2 cells with constitutive NF-κB activity (top). Fifty micro molar of DHMEQ and GST or GST-RelA fusion protein attaching to GST-binding resin were co-incubated in phosphate-buffered saline for 1 h at 4 °C. The reaction mixture was centrifuged for 1 min at 5000 rpm at 4 °C and the supernatant was isolated as pre-absorption solution. 1×10^5 KMH2 cells were cultured with or without the pre-absorption solution for 5 h at 37 °C with 5% CO_2. Cells were subjected to indirect immunofluorescence analysis with antibody for activated RelA, which recognizes RelA NLS, and FITC-conjugated secondary antibody. Analysis of GST and GST-RelA fusion proteins (bottom). GST or GST-RelA fusion proteins that were attached to the GST-binding resin used for the co-incubation experiment were boiled after mixture with sample buffer. The samples were separated on a polyacrylamide/10% SDS gel and visualized by Comassie brilliant blue G-250 staining.

with p50, almost all of the cells transfected with c-Rel, RelB, or p52 showed a nuclear localization pattern (data not shown). A previous report showed that IκBα associates not only with RelA and p50, but also with c-Rel on the C-terminal side of Rel homology domain (RHD), indicating the possibility that IκBα also associates with p52 and RelB [11]. Therefore, we cotransfected expression plasmids for GFP-fused c-Rel, RelB, or p52 with that for IκBα, which enabled us to observe the TNF-α-dependent change in their distribution. DHMEQ treatment inhibited TNF-α-dependent nuclear localization in the nucleus of c-Rel and RelB, but not that of p52 (Fig. 3B and C). Above observations are in accordance with the difference between the amino acid alignment of c-Rel and RelB, which retains the RelA RSAGSI domain, and that of p52, which has the p50 PSHGGL domain.

Previous observation indicated that DHMEQ also inhibits the localization of p52/RelB in the nucleus [13]. This inhibition can be explained by the inhibitory effect of DHMEQ on RelB. Because not only p50/RelA but also p52/RelB pathway is reported to involved in survival of cancer cells [3,14], the inhibitory effect of DHMEQ on both NF-κB pathways appears to explain its potent effect.

DHMEQ directly targets cysteine 38 of RelA

Previous reports indicate that sequiterpene lactone (parthenolide) and epoxyquinone A monomer (EpM) exert their NF-κB inhibitory effect through cysteine 38 of RelA [15–17]. This cysteine 38 is located within the domain that we identified to be necessary to exert the action of DHMEQ (RelA amino acids 25–50). Therefore, we examined the effect of substitution of RelA cysteine 38 with serine (RelA C38S) on the DHMEQ-mediated inhibition of localization of RelA in the nucleus. As a result, DHMEQ could not inhibit the TNF-α-mediated localization of RelA C38S in the nucleus, suggesting that DHMEQ appears to target cysteine 38 of RelA (Fig. 4A). To obtain further support for the above notion, we examined the effect of DTT, a potent reducing agent, which protects thiol groups in proteins like cysteine from oxidization, on the effect of DHMEQ. As shown in Fig. 4B, pre-treatment of cells with DTT, which may reduce reactive cysteine residues in the target proteins, inhibited the effect of DHMEQ (Fig. 4B). Importantly, the RelA RSAGSI domain (amino acids 41–46) does not contain cysteine, and cysteine 38 is the only cysteine residue within the RelA domain (amino acids 25–50).

To obtain further evidence that DHMEQ directly targets RelA cysteine 38, we performed a competition assay on the effect of DHMEQ using GST-fused wild-type RelA and RelA C38S. Pre-incubation of DHMEQ with wild-type RelA abrogated DHMEQ-mediated localization of wild-type RelA in the nucleus. However, pre-incubation of DHMEQ with RelA C38S failed to abrogate DHMEQ-mediated localization of wild-type RelA in the nucleus (Fig. 4C). Taken collectively, these results indicate that DHMEQ directly targets cysteine 38 of RelA via thiol group.

A possible mechanism of selective action of DHMEQ among NF-κB family proteins

The residue corresponding to cysteine 38 of RelA is conserved among p50, p52, c-Rel, and RelB; however, DHMEQ inhibits the localization of RelA, c-Rel, and RelB in the nucleus, but not that of p50 and p52. This difference might be due to the structural difference between RSAGSI and PSHGGL; the former is conserved among RelA, c-Rel, and RelB and the latter between p50 and p52. We found that pre-incubation of DHMEQ with a mutant form of RelA, whose RSAGSI domain was replaced with the corresponding domain of p50 (PSHGGL), did not abrogate the effect of DHMEQ (data not shown). Collectively, the simplest explanation of our results might be that DHMEQ targets the CEGRSAGSI domain structure, which appears in RelA, c-Rel, and RelB, directly binding to cysteine by recognizing the RSAGSI structure.

We searched for the existence of alignment RelA CEGRSAGSI (amino acids 38–46) in mammalian proteins using the FASTA version 3.4t26 sequence alignment software package. The result indicated that there was no matching amino acid alignment RelA CEGRSAGSI (amino acids 38–46) in mammalian proteins, further suggesting that the target of DHMEQ is very unique to a subset of NF-κB family proteins.

Acknowledgment

This work was supported by Grants-in Aid from the Ministry of Education, Science, and Culture of Japan to Ryouichi Horie.

References

[1] N. Matsumoto, A. Ariga, S. To-e, H. Nakamura, N. Agata, S. Hirano, J. Inoue, K. Umezawa, Synthesis of NF-κB activation inhibitors derived from epoxyquinomicin C, Bioorg. Med. Chem. Lett. 10 (2000) 865–869.
[2] T.D. Gilmore, Introduction to NF-κB: players, pathways, perspectives, Oncogene 25 (2006) 6680–6684.
[3] D.S. Basseres, A.S. Baldwin, Nuclear factor-κB and inhibitor of κB kinase pathways in oncogenic initiation and progression, Oncogene 25 (2006) 6817–6830.
[4] K. Umezawa, Inhibition of tumor growth by NF-κB inhibitors, Cancer Sci. 97 (2006) 990–995.
[5] A. Ariga, J. Namekawa, N. Matsumoto, J. Inoue, K. Umezawa, Inhibition of tumor necrosis factor-α-induced nuclear translocation and activation of NF-κB by dehydroxymethylepoxyquinomicin, J. Biol. Chem. 277 (2002) 24625–24630.
[6] M. Watanabe, M.Z. Dewan, T. Okamura, M. Sasaki, K. Itoh, M. Higashihara, H. Mizoguchi, M. Honda, T. Sata, T. Watanabe, N. Yamamoto, K. Umezawa, R. Horie, A novel NF-κB inhibitor DHMEQ selectively targets constitutive NF-κB activity and induces apoptosis of multiple myeloma cells in vitro and in vivo, Int. J. Cancer 114 (2005) 32–38.
[7] M. Watanabe, T. Ohsugi, M. Shoda, T. Ishida, S. Aizawa, M. Maruyama-Nagai, A. Utsunomiya, S. Koga, Y. Yamada, S. Kamihira, A. Okayama, H. Kikuchi, K. Uozumi, K. Yamaguchi, M. Higashihara, K. Umezawa, T. Watanabe, R. Horie, Dual targeting of transformed and untransformed HTLV-1-infected T cells by DHMEQ, a potent and selective inhibitor of NF-κB, as a strategy for chemoprevention and therapy of adult T-cell leukemia, Blood 106 (2005) 2462–2471.
[8] T.A. Kunkel, K. Bebenek, J. McClary, Efficient site-directed mutagenesis using uracil-containing DNA, Methods Enzymol. 204 (1991) 125–139.
[9] D.B. Smith, K.S. Johnson, Single-step purification of polypeptides expressed in *Escherichia coli* as fusions with glutathione *S*-transferase, Gene 67 (1988) 31–40.
[10] A. Hoffmann, G. Natoli, G. Ghosh, Transcriptional regulation via the NF-κB signaling module, Oncogene 25 (2006) 6706–6716.
[11] M. Latimer, M.K. Ernst, L.L. Dunn, M. Drutskaya, N.R. Rice, The N-terminal domain of IκBα masks the nuclear localization signal(s) of p50 and c-Rel homodimers, Mol. Cell. Biol. 18 (1998) 2640–2649.
[12] H. Guan, S. Hou, R.P. Ricciardi, DNA binding of repressor nuclear factor-κB p50/p50 depends on phosphorylation of Ser337 by the protein kinase A catalytic subunit, J. Biol. Chem. 280 (2005) 9957–9962.
[13] G. Matsumoto, J. Namekawa, M. Muta, T. Nakamura, H. Bando, K. Tohyama, M. Toi, K. Umezawa, Targeting of nuclear factor κB Pathways by dehydroxymethylepoxyquinomicin, a novel inhibitor of breast carcinomas: antitumor and antiangiogenic potential in vivo, Clin. Cancer Res. 11 (2005) 1287–1293.
[14] E. Dejardin, The alternative NF-κB pathway from biochemistry to biology: pitfalls and promises for future drug development, Biochem. Pharmacol. 72 (2006) 1161–1179.
[15] A.J. Garcia-Pineres, V. Castro, G. Mora, T.J. Schmidt, E. Strunck, H.L. Pahl, I. Merfort, Cysteine 38 in p65/NF-κB plays a crucial role in DNA binding inhibition by sesquiterpene lactones, J. Biol. Chem. 276 (2001) 39713–39720.
[16] A.J. Garcia-Pineres, M.T. Lindenmeyer, I. Merfort, Role of cysteine residues of p65/NF-κB on the inhibition by the sesquiterpene lactone parthenolide and *N*-ethyl maleimide, and on its transactivating potential, Life Sci. 75 (2004) 841–856.
[17] M.C. Liang, S. Bardhan, J.A. Porco Jr., T.D. Gilmore, The synthetic epoxyquinoids jesterone dimer and epoxyquinone A monomer induce apoptosis and inhibit REL (human c-Rel) DNA binding in an IκBα-deficient diffuse large B-cell lymphoma cell line, Cancer Lett. 241 (2006) 69–78.
[18] E.W. Harhaj, S.C. Sun, Regulation of RelA subcellular localization by a putative nuclear export signal and p50, Mol. Cell. Biol. 19 (1999) 7088–7095.

Int J Hematol (2008) 88:565–570
DOI 10.1007/s12185-008-0209-x

ORIGINAL ARTICLE

Factors predisposing to HTLV-1 infection in residents of the greater Tokyo area

Kaoru Uchimaru · Yukari Nakamura · Arinobu Tojo · Toshiki Watanabe · Kazunari Yamaguchi

Received: 27 March 2008 / Revised: 26 September 2008 / Accepted: 17 October 2008 / Published online: 26 November 2008
© The Japanese Society of Hematology 2008

Abstract Human T-cell leukemia virus type 1 (HTLV-1) is the etiological agent for adult T-cell leukemia. The geographic distribution of HTLV-1 carriers is quite uneven in Japan and the greatest prevalence is in southwestern Japan. Because many people move from endemic areas to the greater Tokyo area, the geographic distribution might have changed. Therefore, we investigated the factors predisposing to HTLV-1 infection, including birthplace, for 88 HTLV-1-infected individuals in greater Tokyo who visited our outpatient clinic. Of these, 39.5% were born in endemic areas, which include Kyushu/Okinawa, south Shikoku, Kii, Tohoku, and Hokkaido, whereas 38.3% were born in greater Tokyo and the proportion is presumed to be increasing. Half of the HTLV-1 infected individuals in greater Tokyo came from endemic areas, whereas around half of the remaining half was presumed to be involved in sexual transmission from a spouse from an endemic area. Overall, they constituted approximately 70% of the HTLV-1 carriers in greater Tokyo. These migration effects may increase the prevalence of HTLV-1 in the greater Tokyo area: nationwide surveillance is warranted.

Keywords Breast-feeding · Geographic distribution · HTLV-1 carrier · Sexual transmission · Tokyo

K. Uchimaru (✉) · Y. Nakamura · A. Tojo
Department of Hematology/Oncology,
The Institute of Medical Science,
The University of Tokyo, 4-6-1, Shirokane-dai,
Minato-ku, Tokyo 108-8639, Japan
e-mail: uchimaru@ims.u-tokyo.ac.jp

Y. Nakamura
Department of Internal Medicine,
Choufu Touzan Hospital, Tokyo, Japan

T. Watanabe
Department of Medical Genome Sciences,
Graduate School of Frontier Sciences,
The University of Tokyo, Tokyo, Japan

K. Yamaguchi
Department of Safety Research on Blood and Biological Products, National Institute of Infectious Disease, Tokyo, Japan

1 Introduction

Human T-cell leukemia virus type 1 (HTLV-1) is the etiological agent for adult T-cell leukemia (ATL) [1] and other diseases, including HTLV-1-associated myelopathy/tropical spastic paraparesis (HAM/TSP) [2] and HTLV-1 uveitis/HTLV-1-associated uveitis (HU/HAU) [3]. In HTLV-1 transmission, breast-feeding plays a major role in mother-to-child transmission and some cases are infected through sexual transmission [4–7]. There are several endemic regions in the world, including Japan [8], specifically southwestern Japan, including Okinawa, Kyushu, and southern Shikoku, although the geographic distribution is quite uneven [9]. A previous nationwide survey of Japan found that 77.9% of ATL patients were born in southern Japan (Kyushu, Kii, and South Shikoku), whereas 9.5% were born in Tohoku and Hokkaido, in northern Japan, which is another endemic area. Only 2.9% were from Kanto district which includes Tokyo, and metropolitan Tokyo was not regarded as an endemic region [9]. The geographic distribution of HTLV-1 carriers might be changing as people continue to move to metropolitan Tokyo from endemic regions. From the perspective of public health, it is important to evaluate the prevalence and distribution of HTLV-1 infection accurately, although no study has examined the geographic distribution of ATL patients in Japan since 1983. Therefore, we investigated the

factors predisposing to HTLV-1 infection, including birthplace, in HTLV-1-infected individuals in metropolitan Tokyo who visited our outpatient clinic. These data are useful for determining the future prevalence of HTLV-1 infection in this area.

2 Subjects and methods

Between March 2006 and December 2007, 107 HTLV-1 infected individuals visited the outpatient clinic at The Research Hospital, The Institute of Medical Science, The University of Tokyo, for a consultation regarding their concerns about HTLV-1 infection or to join a cohort study of HTLV-1 carriers [Joint Study of Predisposing Factors for ATL Development (JSPFAD), supported by the Ministry of Education, Culture, Sports, Science, and Technology of Japan]. Of the 107 individuals, 88 resided in greater Tokyo, which includes Metropolitan Tokyo and Kanagawa, Chiba, Saitama, Tochigi, Gunma, and Ibaraki Prefectures. We investigated the birthplace and other predisposing factors that might be related to HTLV-1 infection in these cases and their families by reviewing their medical records and an inquiry form. We defined Kyushu, south Shikoku, Kii, Tohoku and Hokkaido as endemic areas in Japan [9]. Approval was obtained from the institutional review board. Informed consent was obtained according to the Declaration of Helsinki.

3 Results

3.1 Subject characteristics (Table 1)

Of the subjects, 73 individuals were asymptomatic HTLV-1 carriers, whereas six had HAM, and one had HU. Eight individuals had already developed ATL: three had the smoldering type, three had the chronic type, one had the lymphoma type, and one had the acute type. The sex distribution showed female dominance, with a male/female ratio of 3:5. The majority of cases were in their 30s to 50s and 13 cases (14.8%) were >60 years old.

The most common reason HTLV-1-infected individuals were checked for anti-HTLV-1 antibody was a blood donation at a Japanese Red Cross Blood Center; 36 individuals (40.9%) were identified as anti-HTLV-1 antibody (+) when they donated blood. The next most common reasons were pregnancy ($n = 18$; 20.5%) and having an HTLV-1-infected spouse or relative ($n = 17$; 19.3%). Twelve cases (13.6%) were diagnosed with HTLV-1 infection only when they developed HTLV-1-associated disease. Considering only individuals <40 years old, the proportions diagnosed as HTLV-1 carriers on blood donation and pregnancy increased to 50.0 and 35.7%, respectively (data not shown).

Table 1 Characteristics of visitors to the outpatient clinic for HTLV-1-infected individuals residing in the greater Tokyo area

Characteristic	Category	Number of individuals (total $n = 88$)
Age (years)	21–30	4
	31–40	24
	41–50	26
	51–60	21
	61–70	9
	71–80	4
Sex	Male	32
	Female	56
HTLV-1 disease status	Carrier	73
	HAM	6
	HU	1
	ATL	
	Smoldering	3
	Chronic	3
	Lymphoma	1
	Acute	1
Reason for anti-HTLV-1 antibody testing	Blood donation	36
	Pregnancy	18
	HTLV-1-infected spouse or relative	17
	Developed HTLV-1-associated disease	12
	Visited hospital for a disease unrelated to HTLV-1	4
	Unknown	1

3.2 Birthplaces of HTLV-1 infected individuals and their mothers in greater Tokyo

We examined the geographic distribution of the birthplaces of the subjects and their mothers (Tables 2, 3). Thirty-two cases (39.5%) of HTLV-1-infected individuals in greater Tokyo had moved from endemic areas, and 31 cases (38.3%) were born in the greater Tokyo area. More subjects' mothers were born in endemic areas than the subjects. Forty-five (57.0%) of the mothers of HTLV-1-infected individuals in greater Tokyo were born in endemic areas, whereas only 13 (16.5%) mothers were born in greater Tokyo. The number of subjects' mothers born in greater Tokyo was less than half the number of subjects who were born greater Tokyo.

Table 2 Birthplaces of HTLV-1-infected individuals in the greater Tokyo area

Area of birth	Subjects (%)
Hokkaido/Tohoku	9 (11.1)
Tokyo metropolitan	31 (38.3)
Chubu	10 (12.3)
Hokuriku	1 (1.2)
Kinki	3 (3.7)
Chugoku/north Shikoku	2 (2.5)
Kii/south Shikoku	3 (3.7)
Kyushu	20 (24.7)
Other	2 (2.5)
Total	81 (100)
Unknown	7

Hokkaido/Tohoku, Kii/South Shikoku and Kyushu were defined as endemic

Table 3 Birthplaces of mothers of HTLV-1-infected individuals residing in the greater Tokyo

Area of birth	Mothers (%)
Hokkaido/Tohoku	13 (16.5)
Tokyo metropolitan	13 (16.5)
Chubu	12 (15.2)
Hokuriku	0 (0.0)
Kinki	2 (2.5)
Chugoku/north Shikoku	5 (6.3)
Kii/south Shikoku	3 (3.8)
Kyushu	29 (36.7)
Other	2 (2.5)
Total	79 (100)
Unknown	9

3.3 Factors predisposing to HTLV-1 infection in individuals born in greater Tokyo

We also analyzed the mothers, relatives, and spouses of the 31 cases born in greater Tokyo to identify factors that might be related to HTLV-1 infection (Table 4; Fig. 1). Thirteen cases (41.9%) had mothers from endemic areas and five of these mothers were HTLV-1 infected. The rest of the mothers were not examined for anti-HTLV-1 antibodies, although one HTLV-1-infected subject with one of these mothers who were not examined had an HTLV-1 infected sibling. A total of four cases, including this one, had HTLV-1-infected siblings (Fig. 1).

Two cases had husbands who were HTLV-1-infected and were born in endemic areas; one case had a husband who was infected but not born in an endemic area; and three cases had husbands who were born in endemic areas

Table 4 Predisposing factors in 31 HTLV-1-infected individuals born in the greater Tokyo area (see Fig. 1)

Factor	Number of cases (%)
Mother from an endemic area	13 (41.9)
HTLV-1-infected mother	5[a] (16.1)
HTLV-1 infected sibling	4[b] (12.9)
Father from an endemic area	5[c] (16.1)
Husband from an endemic area	5[c] (16.1)
HTLV-1-infected husband	3[d] (9.7)
No factors/Unknown	10 (32.2)

[a] All of the mothers were from endemic areas

[b] Three of the cases had mothers from endemic areas and two of these three mothers were HTLV-1-infected

[c] Two of the five cases with fathers from endemic areas also had mothers from endemic areas, and one also had a mother and a husband from endemic areas

[d] Two of the cases were from endemic areas, and the birthplace was unknown in one case

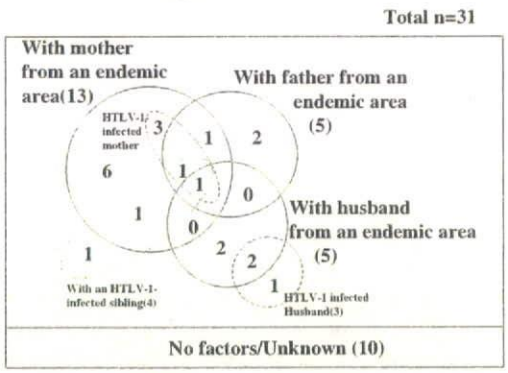

Fig. 1 Schematic presentation of the predisposing factors for 31 HTLV-1-infected individuals born in greater Tokyo. Thirteen cases born in greater Tokyo had mothers from endemic areas, five of whom were HTLV-1 infected. One more case was presumed to have an HTLV-1-infected mother because he had an HTLV-1-infected sibling. In seven cases, a father or a husband from an endemic area or an HTLV-1-infected husband was the only factor predisposing to HTLV-1 infection

and not examined for HTLV-1 antibodies. Among the latter three cases, one case had both a father and mother from an endemic area, and the mother was HTLV-1-infected. Thus, six cases (19.4%) had husbands who were HTLV-1 infected and/or were born in endemic areas (Fig. 1), and in five of these cases (16.1%), the only factor predisposing to HTLV-1 infection was a husband who was HTLV-1 infected or was born in an endemic area.

Two cases had a father and mother from endemic areas, and one had a father, mother, and husband from endemic areas. Two of these three mothers were HTLV-1 infected. Two cases had only a father from an endemic area, making

Table 5 HTLV-1-infected subjects categorized by their and their mother's birthplaces

Birthplace of subjects	Birthplace of their mothers	Number of cases
Endemic area	Endemic area	26
	Non-endemic area	4
	Unknown	2
Non-endemic area	Endemic area	15
	Non-endemic area	30
	Unknown	4
Unknown		7

that the only factor predisposing to HTLV-1 infection in those two cases (Fig. 1). Overall, seven of 17 individuals born in the greater Tokyo area who did not have a mother from an endemic area or an HTLV-1 infected sibling had a husband who was from an endemic area or HTLV-1 infected or a father from an endemic area as the only predisposing factor.

3.4 Factors predisposing to HTLV-1 infection in individuals from non-endemic areas

To further estimate predisposing factors in HTLV-1-infected individuals from non-endemic areas, including greater Tokyo, we analyzed HTLV-1-infected individuals born in non-endemic areas whose mothers were also born in non-endemic areas. As shown in Table 5, the total number of HTLV-1-infected subjects who were from non-endemic areas and whose mothers were also from non-endemic areas was 30 subjects, 15 of whom were born in the greater Tokyo area. [In the 31 HTLV-1-infected individuals born in the greater Tokyo area, 13 individuals had mothers who were born in endemic areas and three had mothers whose birthplaces were unknown (Table 4 and data not shown).] Seven (23.3%) of the 30 cases had HTLV-1-infected husbands, and one case (3.3%) had a father with ATL (Table 6; Fig. 2). Three individuals had a husband from an endemic area, one of which was diagnosed with ATL, and one had a husband whose mother was from an endemic area. Five cases had fathers from endemic areas, and one of these five also had an HTLV-1-infected husband. A father with ATL was from an endemic area and was included in this category. As a result, eitght individuals had an HTLV-1-infected husband or father and five more individuals had a husband or father from an endemic area. One individual had a husband whose mother was from an endemic area (Fig. 2). These cases represent 46.7% of the 30 subjects from non-endemic areas whose mothers were also from non-endemic areas.

Table 6 Predisposing factors in 30 HTLV-1-infected individuals born in non-endemic areas and with mothers from non-endemic areas (see Fig. 2)

Factor	Number of cases (%)
HTLV-1-infected husband	7 (23.3%)
Husband from an endemic area	3[a] (10.0%)
Husband with mother from an endemic area	1 (3.3%)
Father with ATL	1[b] (3.3%)
Father from an endemic area	5[c] (16.7%)
No factors/unknown	16 (53.3%)

[a] One husband was HTLV-1 infected

[b] This father was from an endemic area

[c] One case also had an HTLV-1-infected husband

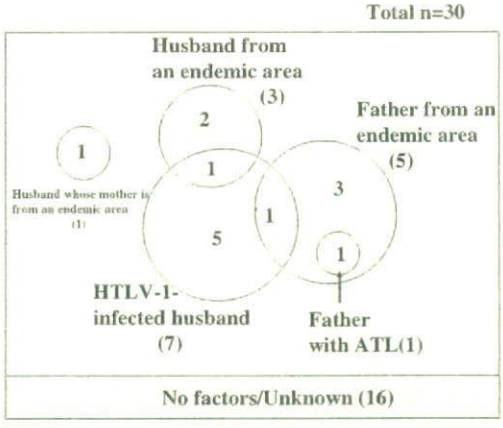

Fig. 2 Schematic presentation of the predisposing factors for 30 HTLV-1-infected individuals born in non-endemic areas with mothers from non-endemic areas. Eight cases had an HTLV-1-infected husband or father. One case had a husband with a mother from an endemic area. There were five more cases who had a husband or a father from an endemic area as the only factor predisposing HTLV-1 infection

4 Discussion

Adult T-cell leukemia is one of the most incurable lymphoid malignancies. The mean survival time of the most commonly used combination of chemotherapies is <1 year [10–13], although a recent prospective randomized study showed some improvement in survival [14, 15]. Several studies have reported promising results of hematopoietic stem cell transplantation, but the study population was small, and the procedure's efficacy remains to be elucidated [16–19]. Given the poor prognosis of ATL, preventing HTLV-1 infection is the most effective strategy for reducing mortality from the disease. In HTLV-1 transmission, breast-feeding plays a major role, and not breast-feeding is shown to be effective in preventing mother-to-child transmission [4, 5]. In endemic areas such

as Kyushu, pregnant women are advised to refrain from breast-feeding, especially in Nagasaki prefecture. Nevertheless, because of the uneven distribution of HTLV-1 carriers in Japan, pregnant women in other areas have received insufficient information on the virus, so it is important from the perspective of public health to determine whether the disease distribution has changed.

Previous nationwide surveys of HTLV-1 carriers based on the rate of anti-HTLV-1 antibody -positive volunteer blood donors [20] and numbers of ATL patients [9] indicated several endemic areas in Japan, including Kyushu and southern Shikoku. In these studies, approximately 55% of HTLV-1 carriers resided in these areas. By contrast, the estimated HTLV-1 prevalence for greater Tokyo was 0.7% [20], which was approximately one-tenth of that for Kyushu, based on the seropositive rate in volunteer blood donors. From these data, greater Tokyo was considered to be a non-endemic area. However, there has been no nationwide survey in the 25 years since these studies, and there is little information on whether the distribution of HTLV-1 carriers has changed with the migration of people to greater Tokyo from endemic areas.

This study investigated the factors predisposing to HTLV-1 infection including the birthplaces of HTLV-1 infected individuals living in greater Tokyo who visited our outpatient clinic to estimate the effect of migration to greater Tokyo. Of 88 HTLV-1-infected individuals in greater Tokyo, approximately 40% of the cases (32 cases) came from endemic areas, whereas almost the same number of individuals were born in greater Tokyo (Table 2). As the number of subjects' mothers born in greater Tokyo was less than half of subjects who were born in greater Tokyo (Table 3), it was assumed that about half of the HTLV-1-infected subjects born in greater Tokyo had mothers from other areas, especially endemic areas. In fact, 41.9% (13 cases) of the 31 subjects born in the greater Tokyo area had mothers from endemic areas (Table 4) and were the offspring of settlers from endemic areas. Of these 13 mothers, 5 were proven to be HTLV-1 infected, and one more mother was very likely HTLV-1 infected because the HTLV-1-infected individual having this mother had an HTLV-1 infected sibling. No mother was proven to be negative for anti-HTLV-1 antibodies. These results make it highly probable that these mothers from endemic areas were HTLV-1 carriers. Fifteen subjects born in non-endemic areas including the 13 cases born in greater Tokyo, had mothers from endemic areas (Table 5).As a result, 47 cases were from endemic areas or had mothers from endemic areas (Table 5) and they constituted 53.4% of the HTLV-1-infected individuals in the greater Tokyo area. These data suggest that more than half of HTLV-1 carriers in greater Tokyo consist of individuals who moved from endemic areas or their offspring. In the fourth nationwide survey [9], 11% of ATL patients resided in Tokyo, although only 2.9% were born there. From these results, we can estimate that 26.3% (2.9/11) of the HTLV-1 carriers in greater Tokyo were born there, which was less than our result (41.9%); this suggests that the second generation of HTLV-1 carriers from endemic areas is increasing in greater Tokyo.

Of the remaining HTLV-1-infected individuals in greater Tokyo, namely cases born in non-endemic areas and with mothers from non-endemic areas (Table 6; Fig. 2), seven cases had HTLV-1-infected husbands and one had an HTLV-1-infected father. This father and one of the husbands were from endemic areas, and the birthplaces of the other four husbands were unknown. There was no HTLV-1-infected husband from greater Tokyo. It is very probable that these cases were infected via sexual transmission from their husbands or involved in mother-to-child transmission from sexually infected mothers because they had no other predisposing factor. Other than these cases, two more husbands were from an endemic area, one other husband had a mother from an endemic area, and three more cases had fathers from endemic areas. As these cases also had no other factors predisposing to HTLV-1 infection, it is probable that they or their mothers were infected via sexual transmission from their spouse, although none of these husbands and fathers was examined for anti-HTLV-1 antibodies. Overall, these cases of possible sexual transmission represent 46.6% (14 cases) of the HTLV-1-infected individuals from non-endemic areas whose mothers were also from non-endemic areas (Fig. 2) and correspond to 15.9% of the HTLV-1-infected individuals in the greater Tokyo area. Combined with the cases who were from endemic areas or had mothers from endemic areas, we estimate that roughly 70% of the HTLV-1 carriers in greater Tokyo came from endemic areas or were infected via sexual transmission from spouses, many of whom were from endemic areas.

Considering only individuals born in greater Tokyo, the only factor predisposing to HTLV-1 infection was a husband or father from an endemic area or an HTLV-1-infected husband in seven cases (Fig. 1), and these cases were probably involved in sexual transmission. They constituted 38.8% of the cases who did not have a mother from an endemic area. Therefore, over 40% of the HTLV-1-infected individuals born in greater Tokyo were assumed to be the offspring of HTLV-1 carrier mothers who moved from an endemic area (Table 4) and around 40% of the remainder were thought to have resulted from sexual transmission. The proportion of possible sexual transmission in cases born in greater Tokyo paralleled that in cases from non-endemic areas with a mother from a non-endemic area, as described above.

Several studies have reported a decline in the prevalence of HTLV-1 [5, 21]. This was explained by the effects of refraining from breast-feeding or lifestyle changes in Japan

such as shortening the period of breast-feeding or having fewer children. Nevertheless, the migration of HTLV-1 carriers from endemic areas could increase the prevalence in the greater Tokyo area, which is regarded as a non-endemic area. In greater Tokyo, most of the HTLV-1 carriers, especially younger ones are diagnosed by chance (Table 1), and they can obtain little information about HTLV-1. An accurate evaluation of the present distribution of the prevalence of HTLV-1 is needed.

Among the subjects of this study, the sex distribution showed female dominance, and the percentage of individuals over 60 years old was relatively low. One possible reason for the female dominance is that female carriers included 18 cases checked for anti-HTLV-1 antibody during pregnancy. Another reason may be that unemployed female carriers such as housewives can visit the outpatient clinic more readily than male carriers. One reason for the relatively low percentage of elderly may be that most of the individuals who visited our hospital had obtained information about our outpatient clinic for HTLV-1 carriers or the JSPFAD study through the Internet, with which elderly individuals are generally unfamiliar. These subject characteristics may have influenced on our results.

In this analysis birthplaces were defined by prefecture. As the distribution of HTLV-1 carriers is uneven, even within a prefecture in some districts, endemic and non-endemic areas are admixed in a prefecture. It is necessary to investigate the birthplace more precisely in order to accurately estimate migration effects.

In conclusion, we surveyed the factors predisposing to HTLV-1 infection in individuals living in the greater Tokyo area and found an effect of migration from endemic areas. Because the distribution of HTLV-1 carriers in Japan has not been explored recently, a nationwide survey of HTLV-1 carriers is warranted.

Acknowledgment This work was supported in part by Grants-in-Aid for Scientific Research from the Ministry of Education, Culture, Sports, Science, and Technology of Japan.

References

1. Yoshida M, Miyoshi I, Hinuma Y. Isolation and characterization of retrovirus from cell lines of human adult T cell leukemia and its implication on the disease. Proc Natl Acad Sci USA. 1982;79:428–37.
2. Osame M, Usuku K, Izumo S, et al. HTLV-I associated myelopathy, a new clinical entity. Lancet. 1986; 1031–2.
3. Mochizuki M, Watanabe T, Yamaguchi K, et al. HTLV-1 uveitis: a distinct clinical entity caused by HTLV-1. Jpn J Cancer Res. 1992;83:236–9.
4. Kinoshita K, Yamanouchi K, Ikeda S, et al. Oral infection of a common marmoset with human T-cell leukemia virus type-I (HTLV-I) by inoculating fresh human milk of HTLV-I carrier mothers. Jpn J Cancer Res. 1985;76:1147–53.
5. Hino S. Primary prevention of adult T cell leukemia (ATL) in Nagasaki, Japan by refraining from breast-feeding. In: Sugamura K, Uchiyama T, Matsuoka M, et al., editors. "Gann Monograph on Cancer Research", No 50. Tokyo: Japan Science Society Press; 2003. p. 241–51.
6. Stuver S, Tachibana N, Okayama A, et al. Heterosexual transmission of human T cell leukemia/lymphoma virus type I among married couples in southwestern Japan: an initial report from Miyazaki cohort study. J Infect Dis. 1993;167:57–65.
7. Iga M, Okayama A, Stuver S, et al. Genetic evidence of transmission of human T cell lymphoma virus type I between spouses. J Infect Dis. 2002;185:691–5.
8. Proietti FA, Carneiro-Proietti ABF, Catalan-Soares BC, et al. Global epidemiology of HTLV-1 infection and associated disease. Oncogene. 2005;24:6058–68.
9. Tajima K, The T- and B-cell malignancy study group and co-authors. The fourth nation-wide study of adult T-cell leukemia/lymphoma (ATL) in Japan: estimates of risk of ATL and its geographical and clinical. Int J Cancer. 1990;45:237–43.
10. Shimoyama M, Ota K, Kikuchi M, et al. Chemotherapeutic results and prognostic factors in patients with advanced non-Hodgkin's lymphoma treated with VEPA and VEPA-M. J Clin Oncol. 1988;6:128–41.
11. Tobinai K, Shimoyama M, Minato K, et al. Japan Clinical Oncology Group phase II trial of second-generation "LSG4 protocol" in aggressive T-and B-lymphoma: a new predictive model for T-and B-lymphoma. Proc Am Soc Clin Oncol. 1994;13:378. (abstr).
12. Tsukasaki K, Tobinai K, Shimoyama M, et al. Deoxycoformycin containing combination chemotherapy for adult T-cell leukemia-lymphoma: Japan Clinical Oncology Group Study (JCOG9109). Int J Hematol. 2003;77:164–70.
13. Taguchi H, Kinoshita K, Takatsuki K, et al. An Intensive chemotherapy of adult T-cell leukemia/lymphoma: CHOP followed by etoposide, videsine, ranimustine, and mitoxantrone with granulocyte colony-stimulating factor support. J Acquir Immune Syndr Hum Retrovirol. 1996;12:182–6.
14. Yamada Y, Tomonaga M, Fukuda H, et al. A new G-CSF-supported combination chemotherapy, LSG15, for adult T-cell leukemia-lymphoma: Japan Clinical Oncology Group Study 9303. Br J Haematol. 2001;113:375–82.
15. Tsukasaki K, Utsunomiya A, Fukuda H, et al. VCAP-AMP-VECP compared with biweekly CHOP for adult T-cell leukemia-lymphoma: Japan Clinical Oncology Group Study JCOG9801. J Clin Oncol. 2007;25:5458–64.
16. Utsunomiya A, Miyazaki Y, Takatsuka Y, et al. Improved outcome of adult T cell leukemia/lymphoma with allogeneic hematopoietic stem cell transplantation. Bone Marrow Transplant. 2001;27:15–20.
17. Kami M, Hamaki T, Miyakoshi S, et al. Allogeneic haematopoietic stem cell transplantation for the treatment of adult T-cell leukemia/lymphoma. Br J Haematol. 2003;120:304–9.
18. Fukushima T, Miyazaki Y, Honda S, et al. Allogeneic hematopoietic stem-cell transplantation provides sustained long-term survival for patients with adult T-cell leukemia/lymphoma. Leukemia. 2005;19:829–34.
19. Okamura J, Utsunomiya A, Tanosaki R, et al. Allogeneic stem-cell transplantation with reduced conditioning intensity as a novel immunotherapy and antiviral therapy for adult T-cell leukemia/lymphoma. Blood. 2005;105:4143–5.
20. Maeda Y, Furukawa M, Takehara Y, et al. Prevalence of possible adult T-cell leukemia virus-carriers among volunteer blood donors in Japan: a nation-wide study. Int J Cancer. 1984;33:717–20.
21. Yamaguchi K, Nishimura Y, Kusumoto Y, et al. Declining trends of HTLV-1 prevalence among blood donors in Kumamoto, Japan. J AIDS. 1992;5:533–4.

From www.bloodjournal.org by on March 22, 2009. For personal use only.

Molecular allelokaryotyping of pediatric acute lymphoblastic leukemias by high-resolution single nucleotide polymorphism oligonucleotide genomic microarray

Norihiko Kawamata,[1] Seishi Ogawa,[2] Martin Zimmermann,[3] Motohiro Kato,[2] Masashi Sanada,[2] Kari Hemminki,[4] Go Yamatomo,[2] Yasuhito Nannya,[2] Rolf Koehler,[5] Thomas Flohr,[5] Carl W. Miller,[1] Jochen Harbott,[6] Wolf-Dieter Ludwig,[7] Martin Stanulla,[3] Martin Schrappe,[6] Claus R. Bartram,[5] and H. Phillip Koeffler[1]

[1]Department of Hematology, Oncology, Cedars-Sinai Medical Center/University of California at Los Angeles School of Medicine; [2]Regeneration Medicine of Hematopoiesis, University of Tokyo, School of Medicine, Tokyo, Japan; [3]Department of Pediatric Hematology and Oncology, Children's Hospital, Hannover Medical School (MHH), Hannover, Germany; [4]Division of Molecular Genetic Epidemiology, German Cancer Research Center (DKFZ), Heidelberg, Germany; [5]Institute of Human Genetics, University of Heidelberg, Heidelberg, Germany; [6]Department of Pediatric Hematology and Oncology, Justus Liebig University, Gießen, Germany; [7]Department of Hematology, Oncology and Tumor Immunology, Robert-Rössle-Clinic at the HELIOS-Clinic Berlin-Buch, Charité, Berlin, Germany; and [8]Department of Pediatrics, University of Kiel, Kiel, Germany

Pediatric acute lymphoblastic leukemia (ALL) is a malignant disease resulting from accumulation of genetic alterations. A robust technology, single nucleotide polymorphism oligonucleotide genomic microarray (SNP-chip) in concert with bioinformatics offers the opportunity to discover the genetic lesions associated with ALL. We examined 399 pediatric ALL samples and their matched remission marrows at 50 000/250 000 SNP sites using an SNP-chip platform. Correlations between genetic abnormalities and clinical features were examined. Three common genetic alterations were found: deletion of *ETV6*, deletion of *p16INK4A*, and hyperdiploidy, as well as a number of novel recurrent genetic alterations. Uniparental disomy (UPD) was a frequent event, especially affecting chromosome 9. A cohort of children with hyperdiploid ALL without gain of chromosomes 17 and 18 had a poor prognosis. Molecular allelokaryotyping is a robust tool to define small genetic abnormalities including UPD, which is usually overlooked by standard methods. This technique was able to detect subgroups with a poor prognosis based on their genetic status. (Blood. 2008;111:776-784)

© 2008 by The American Society of Hematology

Introduction

Pediatric acute lymphoblastic leukemia (ALL) is the most common malignant disease in children.[1-3] ALL is a genetic disease resulting from accumulation of mutations of tumor suppressor genes and oncogenes.[1-3] Knowledge of these mutations can be of use for diagnosis, prognosis, and therapeutic clinical purposes, as well as to provide an overall understanding of the pathogenesis of ALL.[1-3] Identification of mutated genes in ALL has evolved with improvement in technology. A recent approach is single nucleotide polymorphism (SNP) analysis using an array-based technology[4,5] that allows identification of amplifications, deletions, and allelic imbalance, such as uniparental disomy (UPD [represents the doubling of the abnormal allele due to somatic recombination or duplication and loss of the other normal allele]).[6-8] However, since this technique detects allelic dosage, it cannot detect balanced translocations.

According to the HapMap publication, 9.2 million SNPs have been reported, and of these, 3.6 million have been validated.[9] Global genomic distribution of SNPs and its easy adaptability for high throughput analysis make them the target of choice to look for genomic abnormalities in ALL and other cancers.[5-7]

Recently, higher resolution SNP-chip (50 000-500 000 probes) has been developed for large-scale SNP typing.[4,10] With a large number of SNP probes, in combination with the algorithms specifically developed for copy number calculations, these SNP-chips enable genomewide detection of copy number changes.[11,12] The combination of SNP-chip technology, nucleotide sequencing, and bioinformatics allows the investigator to view the entire genome of ALL in an unbiased, comprehensive approach. Using SNP-chips, the chromosomal abnormalities can be evaluated at a very high resolution (molecular level: average distances of each probe are 47 kb and 5.8 kb in the 50 k/500 k arrays, respectively[4,10]), and allele-specific gene dosage level (gene dosage of paternal and maternal alleles) also can be analyzed in the whole genome.[11,12] Hence, we name this new technology "molecular allelokaryotyping."[12] In this study, we performed molecular allelokaryotyping on a very large cohort (399) of pediatric ALL samples to examine genomic abnormalities at high resolution. Further, we examined correlations between the genomic abnormalities detected by SNP-chip and clinical features, including prognosis.

Submitted May 1, 2007; accepted September 13, 2007. Prepublished online as *Blood* First Edition paper, September 21, 2007; DOI 10.1182/blood-2007-05-088310.

N.K., S.O., and M.Z. equally contributed to this work as first authors. C.R.B. and H.P.K. equally contributed to this work as last authors.

An Inside *Blood* analysis of this article appears at the front of this issue.

The online version of this article contains a data supplement.

The publication costs of this article were defrayed in part by page charge payment. Therefore, and solely to indicate this fact, this article is hereby marked "advertisement" in accordance with 18 USC section 1734.

© 2008 by The American Society of Hematology

From www.bloodjournal.org by on March 22, 2009. For personal use only.

Methods

Clinical samples and DNA/RNA preparation

The ALL-BFM 2000 trial of the Berlin-Frankfurt-Münster (BFM) study group on treatment of childhood ALL enrolled patients from ages 1 year to 18 years at diagnosis.

From September 1999 to January 2002, 566 patients were consecutively enrolled in this trial. The ALL-BFM 2000 study was approved by the ethics committees of the Medical School Hanover and the Cedar Sinai Medical Center. Informed consent was obtained in accordance with the Declaration of Helsinki.

Of the 566 patients (nos. 299-854), 399 patients, representing 70% of the entire patient population, had additional DNA available and could be included in the present SNP-chip study. The 167 patients not available for this analysis did not differ from the 399 patients in this study with regard to their clinical and biological characteristics (data not shown).

Complete remission (CR) was defined as the absence of leukemia blasts in the peripheral blood and cerebrospinal fluid, fewer than 5% lymphoblasts in marrow aspiration smears, and no evidence of localized disease. At day 29, bone marrows were examined, and all patients in this SNP-chip analysis study obtained a CR at that time. The remission marrows were collected and used as matched control for the SNP-chip analysis.

Prednisone response was defined based on numbers of peripheral blood blasts per microliter on day 8, and patients were classified into good (< 1000 blasts/μL) and poor responders (≥ 1000 blasts/μL).[13-15] Relapse was defined as recurrence of lymphoblasts or localized leukemic infiltrates at any site.

DNA index, immunophenotyping, molecular analysis of chromosomal abnormalities

Leukemic or normal bone marrow cells were stained with propidium iodide, and cellular DNA contents were measured by cytometric analysis as previously reported.[16,17] DNA index was defined as the DNA content of leukemic cells compared with normal G0/G1 cells. When the DNA index of leukemic cells was the same as or greater than 1.16, it was defined as hyperdiploid ALL by DNA index as previously reported.[16,17]

Immunophenotyping of ALL was examined using anti-CD2, -CD3, -CD4, -CD10, -CD19, and -CD20 antibodies by FACS.[13-15] ETV6/RUNX1, BCR/ABL, and MLL/AF4 were examined by interphase fluorescence in situ hybridization (FISH) analysis using specific probes and by reverse transcriptase–polymerase chain reaction (RT-PCR) using specific primers for these fusion transcripts as described previously.[13-15]

Molecular allelokaryotyping of leukemic cells

DNA from the 399 ALL samples as well as their paired normal DNA from remission samples were analyzed on Affymetrix GeneChip human mapping 50 K *Xba*I or 250 K Nsp arrays (Affymetrix Japan, Tokyo, Japan) according to the manufacturer's protocol. Microarray data were analyzed for determination of both total and allelic-specific copy numbers using the CNAG program as previously described[11,12] with minor modifications, where the status of copy numbers as well as UPD at each SNP was inferred using the algorithms based on Hidden Markov Models.[11,12]

For clustering of ALL samples with regard to the status of copy number changes as well as UPD, entire genome was divided into contiguous sub-blocks of 100 kb in length, and according to the inferred copy numbers (CNs) and the status of UPD, one of the 4 conditions was assigned to the *i*th sub-block (*Si*): CN gain, CN loss, normal CN, and UPD. For a given 2-copy number data, A and B, distance (d[A,B])was simply defined as

$$d(A,B) = \sum_i \mathrm{I}(S_i^A; S_i^B)$$

$$\mathrm{I}(S_i^A; S_i^B) = \begin{cases} 1 \text{ if } S_i^A = S_i^B \\ 0 \text{ if } S_i^A \neq S_i^B \end{cases}$$

where S_i^A and S_i^B are the status of the *i*th sub-block (*Si*) in data A and B, respectively, and sum is taken for all sub-blocks. Clustering was initiated by finding a seed cluster of 2 samples showing the minimum distance and replacing them with the cluster data having the mean *Si* value of the two. This procedure was iteratively performed until all samples were converged to one cluster based on this distance using a program developed for this purpose (GNAGraph), which was followed by manual revisions focusing on particular genetic lesions selected by their frequencies within the sample set. CNAG and CNAGraph are available on request.

Quantitative genomic PCR and direct sequencing

Quantitative genomic PCR (qPCR) was performed on a real-time PCR machine, iCycler (Bio-Rad Laboratories, Hercules, CA) using iQ cybergreen supermix (Bio-Rad Laboratories) according to the manufacturer's protocol. Primer sequences used for the qPCR are listed in Table S2 (available on the *Blood* website; see the Supplemental Materials link at the top of the online article). Gene dosage at the 2p allele was used as an internal control. Allelic gene dosage of 9p and 9q was measured, and these were compared with the levels in respective matched control DNA. SNP sites were amplified and directly sequenced on Autosequencer 3000 (Applied Biosystems, Foster City, CA). Primers used for SNP site amplification are listed in Table S2. Exons 12 and 14 of JAK2 gene were amplified as previously reported.[18] PCR products were purified and subjected to direct sequencing.

Data preparation

Proportional differences between groups were analyzed by either chi-squared (χ^2) or Fisher exact tests. The Kaplan-Meier method was used to

Table 1. Characterization of clinical features of 399 ALL cases

	Cases, no. (%)
Sex	
Male	230 (57)
Female	169 (43)
Age	
1 to 9 yrs	307 (77)
Older than 10 yrs	92 (23)
WBC	
Below $10^2 \times 10^9$/L	362 (91)
Over $10^2 \times 10^9$/L	37 (9)
Immunophenotype	
T-cell	49 (12)
B-cell	339 (85)
Unknown	11 (3)
CNS involvement	
Yes	11 (3)
No	358 (90)
unknown	30 (7)
BCR/ABL	
Yes	6 (2)
No	379 (95)
Unknown	14 (3)
ETV6/RUNX1	
Yes	96 (24)
No	270 (68)
Unknown	33 (8)
PDN response	
Good	360 (90)
Poor	35 (9)
Unknown	4 (1)

WBC indicates white blood cell count ($\times 10^9$/L) in peripheral blood at diagnosis; CNS involvement, central nervous system involvement at diagnosis; *BCR/ABL* and *ETV6/RUNX1*, *BCR/ABL* or *ETV6/RUNX1* fusion was examined by RT-PCR and/or FISH analysis; PDN, prednisone; and PDN response, blast cell count was 1000/μL or greater in peripheral blood after a 7-day exposure to prednisone and one intrathecal dose of methotrexate.

From www.bloodjournal.org by on March 22, 2009. For personal use only.

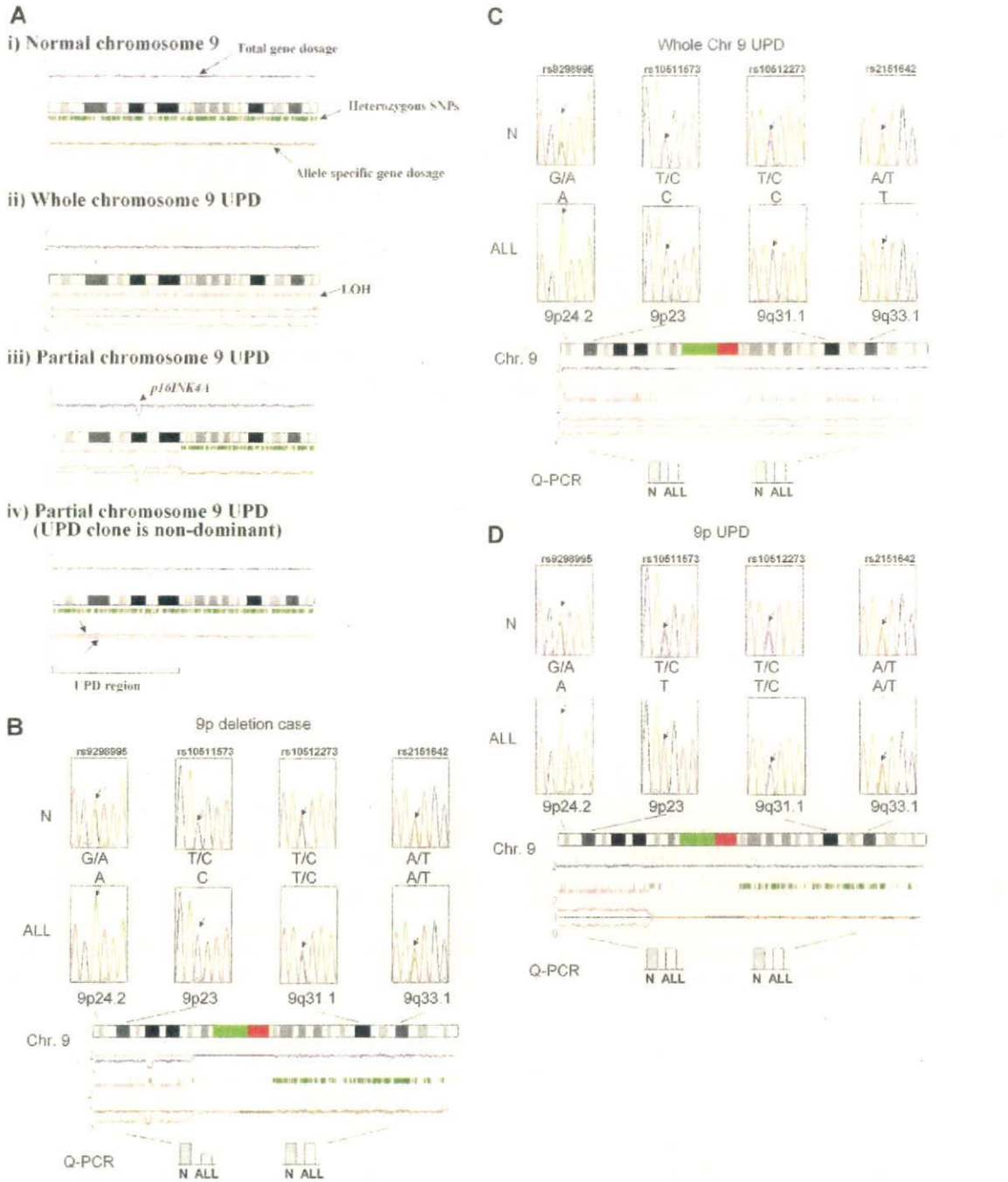

Figure 1. Result of SNP-chip analysis. (A) Results of normal and abnormal chromosomes visualized by CNAG software. Blue lines above each chromosome show total gene dosage; level 2 indicates diploid (2N) amount of DNA, which is normal. Green bars under each chromosome indicate the SNP sites showing heterozygosity in leukemic cells. When heterozygosity is not detected in the leukemic cells but is detected in matched normal controls, the result suggests that the leukemic cells have allelic imbalance (AI) in that region. Pink bars that replaced green ones suggest AI. The bottom lines (green and red lines) in each panel show allele-specific gene dosage levels (one indicates the gene dosage of paternal allele, the other indicates the gene dosage of maternal allele). Level 1 is normal for each gene dosage. (i) Pattern of normal chromosome 9. Blue line is at level 2 (2N DNA). Large number of SNP sites shows normal heterozygosity (green bars under the chromosomes), and no pink bars are detected. Allele-specific gene dosage is at level 1. Panel ii shows the pattern of whole chromosome 9 uniparental disomy (UPD) detected by SNP-chip. Total gene dosage (blue line) is normal (level 2). A number of pink bars (AI) are detected. Allele-specific gene dosage data show that one allele is deleted (level 0) and the other allele is duplicated (level 2). Panel iii shows the pattern of partial UPD. Left half shows the pattern of UPD as described above. Right half shows the pattern of a normal chromosome as described above. This case also has homozygous deletion of *p16INK4A* gene (see that both allele-specific dosage lines [green and red lines] and total gene dosage line [blue line] are at zero). Panel iv shows nondominant UPD. Total gene dosage (blue line) indicates 2N. Allele-specific gene dosage lines (arrows, green and red lines) on left half show that one allele (green line) is lower than normal, and the other allele (red line) is higher than normal. Allele-specific gene dosage on right half show that each allele has same level. (B-D) Validation of SNP-chip data by direct nucleotide sequencing of SNP sites and qPCR. Top panels: direct nucleotide sequencing of SNP sites in ALL samples with matched controls. ALL indicates leukemic samples; N, matched control samples. Heterozygous SNP sites are indicated by arrows. Middle panels: results of SNP-chip data (see Figure 1 legend). Bottom panels: qPCR at each chromosome location. Gene dosage levels were examined using qPCR at indicated chromosomal region. Gene dosage was determined relative to the levels at the 2p21 region. Gene dosage in leukemic cells (ALL) was compared with the matched normal control DNA (N). (B) ALL with 9p hemizygous deletion; homozygous deletion of 9p21 is also detected. (C) ALL with whole chromosome UPD. (D) ALL with 9p UPD.

From www.bloodjournal.org by on March 22, 2009. For personal use only

Table 2. Detection of hyperdiploidy ALL by DNA-index and SNP-chip analysis

	SNP-chip	
	HD	non-HD
DNA index		
HD	44 cases	4 cases
non-HD	30 cases	200 cases

DNA index was measured by FACS as described in "DNA index, immunophenotyping, molecular analysis of chromosomal abnormalities" and DNA index of 278 ALL samples were available. Normal diploid cells have a DNA index of 1.0. When DNA index is the same as or greater than 1.16, the leukemia is defined as hyperdiploid ALL by DNA index. Hyperdiploid ALL detected by SNP-chip analysis had more than 50 chromosomes, which were counted manually.

HD indicates hyperdiploid ALL; and non-HD, nonhyperdiploid ALL.

estimate survival rates. Differences were compared with the 2-sided log-rank test. Event-free survival (EFS) was calculated from diagnosis to the time of the first event (relapse, secondary malignancy, or death from any cause) or to the date of last follow-up.

Results

Features of samples

Clinical features of 399 pediatric ALL patients are shown in Table 1. Infant ALL (< 1years of age) were excluded from this study, and 77% (307 cases) of the patients were from 1 to 9 years old. Forty-nine cases of T-cell lineage ALL and 339 cases of B-cell lineage ALL were examined. Ninety-six samples (24%) had *ETV6/RUNX1* fusion, and 6 cases had the *BCR/ABL* fusion gene.

Validation of SNP-chip data

Gene dosage, heterozygous SNPs, allele-specific gene dosage, and allelic composition (loss of heterozygosity [LOH]) was visualized as shown in Figure 1 using our novel analysis software, CNAG for SNP-chip.[11,12] Duplication/amplification, deletion, and UPDs of chromosomes were easily detected (Figure 1A). To validate abnormalities found by SNP-chip, genomic quantitative PCR and direct sequencing of SNP sites at duplicated, amplified, deleted, and UPD regions were performed including chromosome 9. Representative results of validation are shown in Figure 1B-D.

Also, hyperdiploid (HD) ALL defined by DNA index and SNP-chip analysis was compared for selected cases (Table 2). Number of total chromosomes was counted manually in SNP-chip analysis, and ALL with more than 50 chromosomes was defined as HD-ALL by SNP-chip. When DNA index of leukemic cells was same as or greater than 1.16, the sample was defined as HD-ALL by DNA index.[16,17] DNA index of 278 ALL samples were available, and 200 cases were defined as non-HD ALL by both methods. SNP-chip detected more cases of HD-ALL (74 cases) than DNA index. As shown in Figure 1Aiv, SNP-chip can precisely detect gene dosage, and this high sensitivity of SNP-chip analysis permitted more accurate detection of HD-ALL than by the DNA index method. Results of these analyses validated that the abnormalities detected by SNP-chip were reliable.

Three common abnormalities in pediatric ALL

Figure 2A summarizes molecular allelokaryotyping profiles of the 399 ALL cases after clustering with regard to the status of copy number alterations as well as copy number neutral LOH, so-called UPD, showing a number of clusters having common genetic lesions.

Among these clusters, 3 genetic abnormalities were frequently detected: hyperdiploidy (HD, > 50 chromosomes), deletion of the 9p region, and deletion of 12p (Figure 2A,B). The common deleted region (CDR) on 9p involved the *p16INK4A* gene (called p16Del, Figure 2B), and the CDR on 12p involved the *ETV6* gene (called ETV6Del, Figure 2B). Concurrent abnormalities of p16Del and HD were rare ($P < .001$); concurrent abnormalities of ETV6Del and HD also were rare ($P < .001$; Figure 2B). No case had all 3 common abnormalities.

The clinical features of cases with each of these 3 genetic abnormalities were analyzed (Table 3). Individuals with p16Del-ALL frequently were older ($P = .017$), had higher WBC ($P < .001$), and T-cell lineage ALL ($P < .001$). Those with ETV6Del-ALL were more often younger ($P = .009$), non–T-cell lineage ($P = .014$), and *ETV6/RUNX1* fusion gene positive ($P < .001$). Patients having HD-ALL were more frequently younger ($P < .001$), showed lower WBC ($P < .001$), non–T-cell lineage ($P < .001$), and *ETV6/RUNX1* negative ($P < .001$).

Numerical chromosomal abnormalities in pediatric ALL

Numerical chromosome changes were frequently detected in pediatric ALL samples, as summarized in Figure 3A. Numerical change of chromosome 21 (trisomy, tetrasomy, and pentasomy) was the most frequent (134 [34%] cases). We had 8 cases with Down syndrome who had trisomy 21 in their leukemic cells and their matched controls. These 8 cases are excluded in Figure 3A. Most of the numerical abnormalities were detected in HD-ALL cases (Figure S1A) except for those with trisomy 21 (Figure S1B). As for trisomy 21, half (21 cases) occurred in patients with subtypes other than HD (Figure S1B). In HD-ALL, gain of chromosomes was restricted to particular chromosomes, involving chromosomes 4, 6, 8, 10, 14, 17, 18, 21, and X (Figures 2A, 3A).

Nonrandom genetic abnormalities in pediatric ALL detected by SNP-chip

All copy number changes (deletions and duplications/amplifications) detected by SNP-chip analysis are shown in Figure 2A and Figure S2. Small deletions that could not be detected by conventional cytogenetics were sensitively identified, including deletions of 3p14.2 (500 kb), 3q26.32 (700 kb), and Xp21.1 (1 Mb) (Table 4 and Figure S2). Nonrandom chromosomal abnormalities (frequency > 1.5% of all cases) are listed in Table 4. Besides the 3 common genetic abnormalities, duplication of 1q (11%) and deletion of 6q (11.5%) were often detected. In 13 cases with 1q duplication, the duplication began at the *PBX1* gene (Figures 2A, S2). Since gain of the entire or part of either chromosome 21 or X was frequently found in non–HD-ALL, these abnormalities were grouped separately (Table 4).

Recently, other groups of investigators performed SNP-chip analysis on pediatric ALL and found deletions of several transcriptional factors associated with B-cell development including *PAX5* (9p13), *EBF* (5q33), *Ikaros* (7p12.2), *Aiolos* (17q12), *LEF1*(4q25), *RAG1*(11p12), and *RAG2* (11p12).[19,20] We also have found deletion of these genes in our study. However, the frequency of deletion of these genes, except for PAX5, was low (fewer than 2%) and/or the deleted regions contained multiple genes (Table 4; Figure S2 and data not shown).

UPD

One of the major advantages of SNP-chip analysis is capability of sensitive detection of UPD, even in samples suffering from small